## USE OF VARIOUS COMPUTATIONAL SOFTWARE BY STUDENTS IN PROJECT AND PUBLICATION

| Sr. No | Name of Student | Software | Project Title |
|---|---|---|---|
| 1 | Anjali Bhoyar | Chemsketch and Docking software | Computational guided biological activity of novel substituted Indolizine-7-carbonitrile derivatives |
| 2 | Rohini Kharwade | Chemsketch, Mendeley referencing | Starburst PAMAM dendrimers: Synthetic approaches, surface modifications, and biomedical applications |
| 3 | Jayashri Kumare | Chemsketch and docking software | In silico Antidiabetic characterization and ADME studies of Swertia chirality |
| 4 | Khushbu Pandhare | Chemsketch and Docking software | In silico studies of phytomedicines for CoVID-19 |
| 5 | Mayur Mahajan | Chemsketch and Docking software | Design of 2-amino-4-chlorophenol Schiff base metal complex for COVID-19 disease: an in-silico approach |
| 6 | Priyanka Yadav | Chemsketch and Docking software | Design, synthesis, pharmacological evaluation and In-silico studies of new 2-oxo-4-substituted aryl azetine benzotriazole derivatives |
| 7 | Rushikesh Bobde | Chemsketch and Docking software | In silico study of abutilon indicum for hypoglycaemic activity |
| 8 | Shatayu Wasnik | ADME software | In silico investigation of aniline Schiff base to target the SARS-COV-2 properties of COVID-19 |
| 9 | Shruti kale | ADME software | In silico Antidiabetic activity of bioactive compounds in pterocarpus marsupium |
| 10 | Shruti Tejekar | ADME software | Computational guided identification of potential phytoconstituent of plant withania coagulans |
| 11 | Kapil Pawar | DOE software version 13 | Development and characterization of gel formulation for Topical application |
| 12 | Rushikesh Harde | DOE software version 13 | Formulation development and evaluation of gastroretentive floating pellets for the improvement of bioavalability |
| 13 | Tirupati Kedar | DOE software version 13 | Formulation of polyherbal emulgel by quality by design (QbD) approach for alopecia |
| 14 | Tushar Mandale | DOE software version 13 | A panchagavya-based herbal nanogel with potential for psoriasis. |
| 15 | Elizabeth Suresh | PKsolver software, Graph pad prism, Chromoleon and LC solution | Improvement in Bioavailability and Pharmacokinetic Characteristics of Efavirenz with Booster Dose of Ritonavir in PEGylated PAMAM G4 Dendrimers |

DADASAHEB BALPANDE COLLEGE OF PHARMACY ★ BESA, NAGPUR-37 ★ SEAL

Mahajan

PRINCIPAL
DADASAHEB BALPANDE COLLEGE
OF PHARMACY, BESA, NAGPUR - 37

# COMPUTATIONAL GUIDED BIOLOGICAL ACTIVITY OF NOVEL SUBSTITUTED INDOLIZINE-7- CARBONITRILE DERIVATIVES

**Project Report**

Submitted in partial fulfilment of the

Requirement for the degree of

**Bachelor of Pharmacy**

In the faculty of Science and Technology,

Rashtrasant Tukadoji Maharaj Nagpur University, Nagpur.

**By**

Miss. Anjali V. Bhoyar

**Guide**

Mr. Kishor Danao

(M.Pharm, DDP)



**Ambe Durga Education Society's**

**Dadasaheb Balpande College of Pharmacy, Besa,**

**Nagpur-440037**

**2021-2022**

Table 3: Various protein with their description

| Sr no. | Protein | Description |
|---|---|---|
| 1. | 6LU7 | The crystal structure of COVID-19 main protease in complex with an inhibitor N3 |
| 2. | 2GIB | Crystal structure of the SARS corona virus nucleocapsid protein dimerization domain |
| 3. | 5XES | TK9 NMR structure in SDS micelle |
| 4. | 5XER | TK9 NMR structure in DPC micelle |
| 5. | 3CL5 | Crystal structure of bovine coronavirus hemagglutinin-esterase |
| 6. | 3CL5 | Structure of coronavirus hemagglutinin-esterase in complex with 4,9-O-diacetyl sialic acid |
| 7. | 7B3E | Crystal structure of myricetin covalently bound to the main protease (3CLpro/Mpro) of SARS-CoV-2 |
| 8. | 7LM9 | Crystal structure of SARS-CoV spike protein receptor-binding domain in complex with a cross-neutralizing antibody CV38-142 Fab isolated from COVID-19 patient |
| 9. | 7LM8 | Crystal structure of SARS-CoV-2 spike protein receptor-binding domain in complex with two cross-neutralizing antibodies CV38-142 and COVA1-16 Fabs isolated from COVID-19 patients |
| 10. | 7LYJ | SARS-CoV-2 frameshifting pseudoknot RNA |
| 11. | 7MKY | SARS-CoV-2 frameshifting pseudoknot RNA |
| 12. | 7LTU | AALALL Segment from the nucleoprotein of SARS-COV-2, residues 217-222, crystal form 1 |
| 13. | 7ACT | The SARS-CoV-2 nucleocapsid phosphoprotein N-terminal domain in complex with 10mer ssRNA |
| 14. | 7ACS | The SARS-CoV-2 nucleocapsid phosphoprotein N-terminal domain in complex with 7mer dsRNA |
| 15. | 2CJR | Crystal structure of oligomerization domain of SARS coronavirus nucleocapsid protein |

## RESULT AND DISCUSSION:

We docked each of the four ligands, namely, 1-benzoyl-2-phenylindolizine-7-carbonitrile, remdesivir, flavipiravir and hydroxychlorquine with our 15 target protein separately by Docking Server. In order to study interaction of the compounds standard drugs (Ramdesivir, Flavipiravir, Hydrochlorquine) and 1-Benzoyl-2-Phenylindolizine-7-Carbonitrile with various proteins we performed docking analysis by pyrx-virtual screening tool. Selected ligands showing best results were further evaluated for absorption, distribution, metabolism, excretion, and toxicological (ADMET) properties using SwissADME and pkCSM online server.

### Molecular docking studies:-

Table 4: - Interaction of ligand with amino acid residue

| Sr No | Protein | Distance Interaction (Å) | Amino Acid Residue |
|---|---|---|---|
| 1. | 6LU7 | 4.61, 4.67, 5.56, 4.86, 5.44 | HIS A:41, MET A:49, MET A:165, HIS A:164, CYS A:145 |
| 2. | 2GIB | 3.91, 3.11 | ALA B:337, GLN A:282 |
| 3. | 5XES | 4.89, 3.72, 3.46, 4.15, 5.22 | TYR A:5, THR A:1, VAL A:4 |
| 4. | 5XER | 4.20, 3.76, 4.24 | VAL A:4, VAL A:8 |
| 5. | 3CL4 | 5.19, 5.43 | PHE A:283, PRO A:310 |
| 6. | 3CL5 | 3.20, 2.91, 4.16 | THR A:114, LEU A:212, PHE A:245 |
| 7. | 2CJR | 5.45, 3.78, 3.61, 3.25, 3.28, 5.30, 3.45 | GLN F:290, ARG F:277, ARG F:278, ARG G:294, ILE F:293, ASN G:270, THR F:272 |
| 8. | 7ACS | 4.71, 4.45, 4.86, 3.76, 4.87, 5.68, 4.11, 4.87 | C C:10, PRO A:111, ALA A:69, TYR A:69, ALA A:10, SER A:11, ALA A:116 |
| 9. | 7ACT | 3.00, 4.60, 5.42, 3.62, 3.51 | ARG A:149, TRP A:52, ILE A:157, ASN A:154, ASN A:150 |
| 10. | 7B3E | 4.84, 5.00, 5.19 | ILE B:249, PRO B:293, VAL B:202 |
| 11. | 7LM8 | 3.11, 4.06, 2.79, 3.65, 3.51, 4.88, 3.50, 5.10 | TYR H:100K, ASP L:50, TYR L:49, VAL A:407, THR A:376, LYS A:378, ARG A:408, ALA A:411 |
| 12. | 7LM9 | 4.07, 3.18, 3.13, 3.10 | LYS L:39, MET H:89, LYS H:43, GLY H:42 |
| 13. | 7LTU | 3.77, 5.12, 5.37 | ALA B:220, LEU A:219, LEU B:222 |
| 14. | 7LYJ | 3.20, 2.99, 4.94, 4.54 | C A:24, A A:23, G A:2 |
| 15. | 7MKY | 5.10, 3.55, 3.49 | C A:34, G A:33, U A:51 |

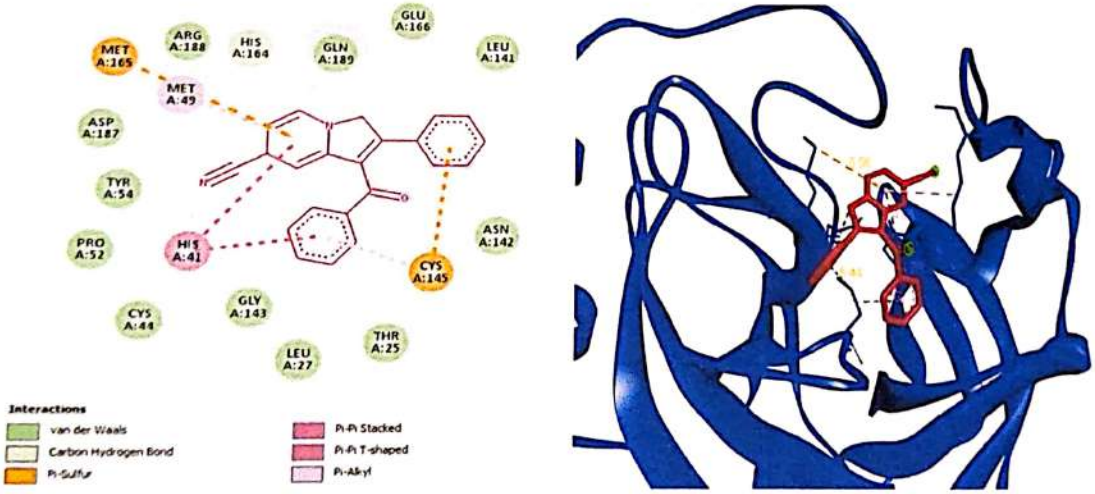


Figure 1: 2D AND 3D STRUCTURE OF 6LU- INDOLIZINE DRUG

1-Benzoyl-2-Phenylindolizine-7-Carbonitrile shows binding energy of -7.7 kcal/mol with 6LU7 protein it makes hydrogen bonding with amino acid HIS164 along with bond length 4.86. It also shows bonding viz. pi-pi stacking, pi-pi sigma with amino acid HIS41 with bond length 4.61. Also, 1-Benzoyl-2-Phenylindolizine-7-Carbonitrile has interacted with amino acid residue MET49 with bond length 4.67 along with the pi-alkyl bond. It also shows bonding via

pi-sulfur with amino acid MET165 and CYS145 with bond length 5.56 and 5.44 respectively shown in figure 1.

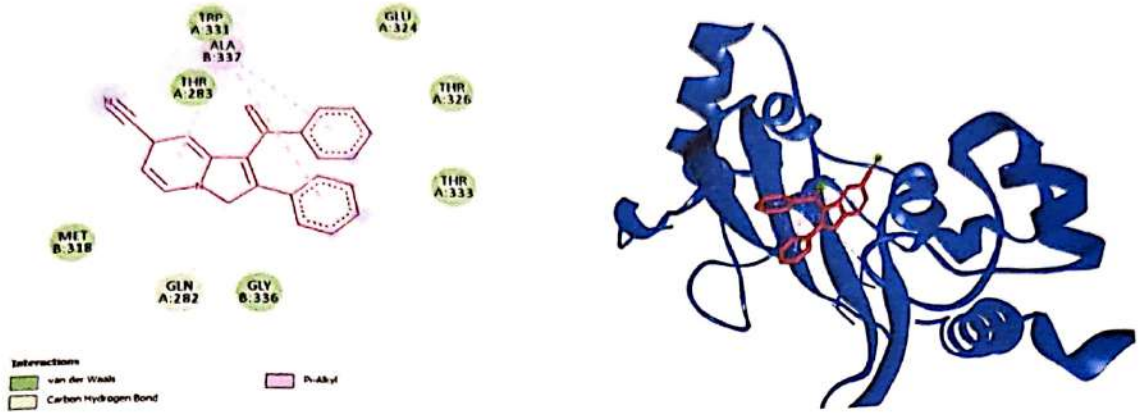


Figure 2: 2D AND 3D STRUCTURE OF 2GIB- INDOLIZINE DRUG

1-Benzoyl-2-Phenylindolizine-7-Carbonitrile shows binding energy of – 8.1 kcal/mol with 2GIB protein it makes hydrogen bonding with amino acid GLN282 along with bond length 4.86. It also shows bonding viz. pi-pi stacking, pi-pi sigma with amino acid HIS41 with bond length 3.11. Also, 1-Benzoyl-2-Phenylindolizine-7-Carbonitrile has interacted with amino acid residue ALA337 with bond length 3.91 along with the pi-alkyl bond shown in figure 2.

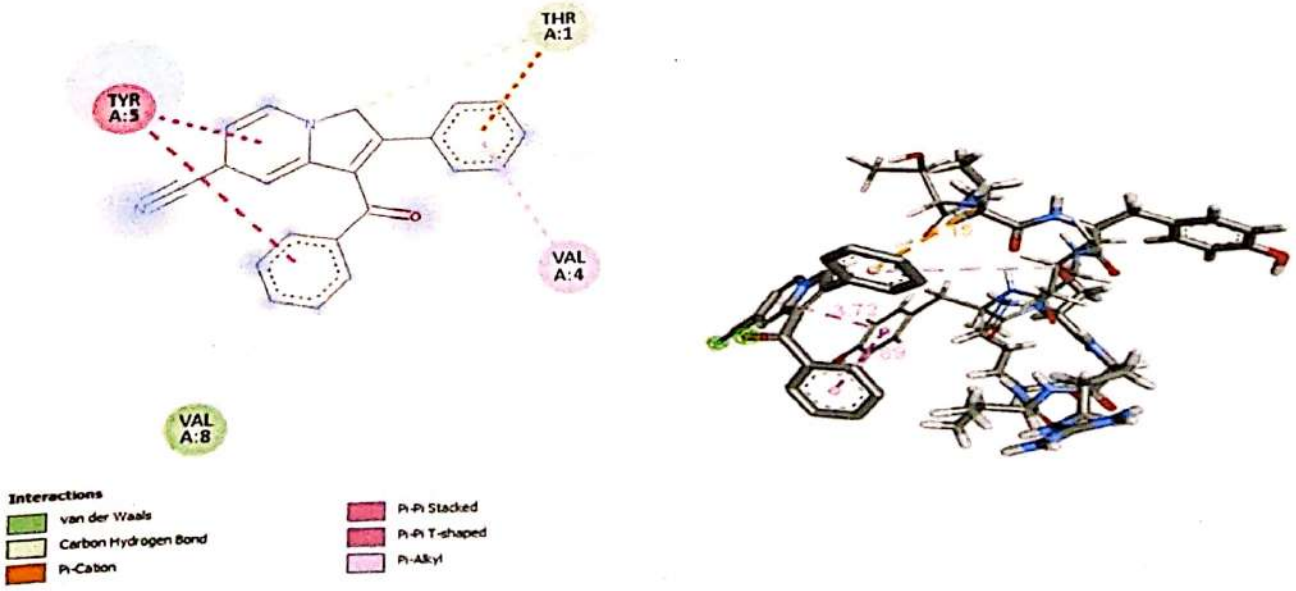


Figure 3: 2D AND 3D STRUCTURE OF 5XES-INDOLIZINE DRUG

1-Benzoyl-2-Phenylindolizine-7-Carbonitrile shows binding energy of -5 kcal/mol with 5XES protein it makes hydrogen bonding with amino acid THR1 along with bond length 3.46. It also shows bonding viz. pi-pi stacking, pi-pi sigma with amino acid THR5 with bond length 4.89 and 3.72. Also, 1-Benzoyl-2-Phenylindolizine-7-Carbonitrile has interacted with amino acid residue VAL4 with bond length 5.22 along with the pi-alkyl bond shown in figure 3.

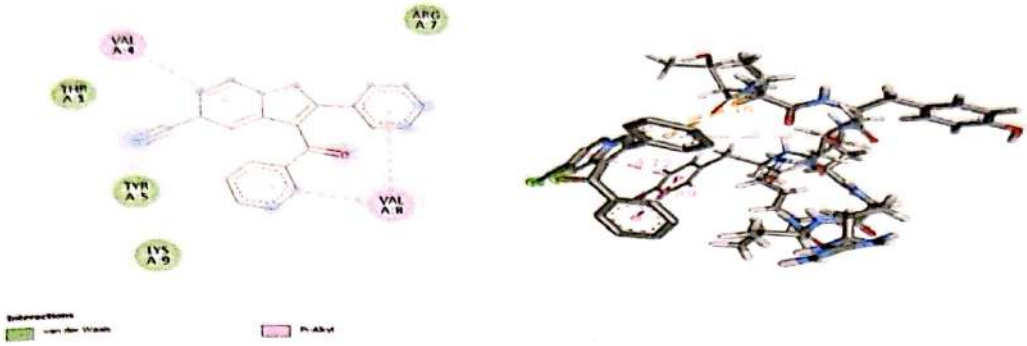


Figure 4: 2D AND 3D STRUCTURE OF 5XER- INDOLIZINE DRUG

1-Benzoyl-2-Phenylindolizine-7-Carbonitrile shows binding energy of -5.8 kcal/mol with 5XER protein it makes pi-alkyl bond with amino acid VAL 4 andVAL8 along with bond length 4.24 and 4.20 shown in figure 4.

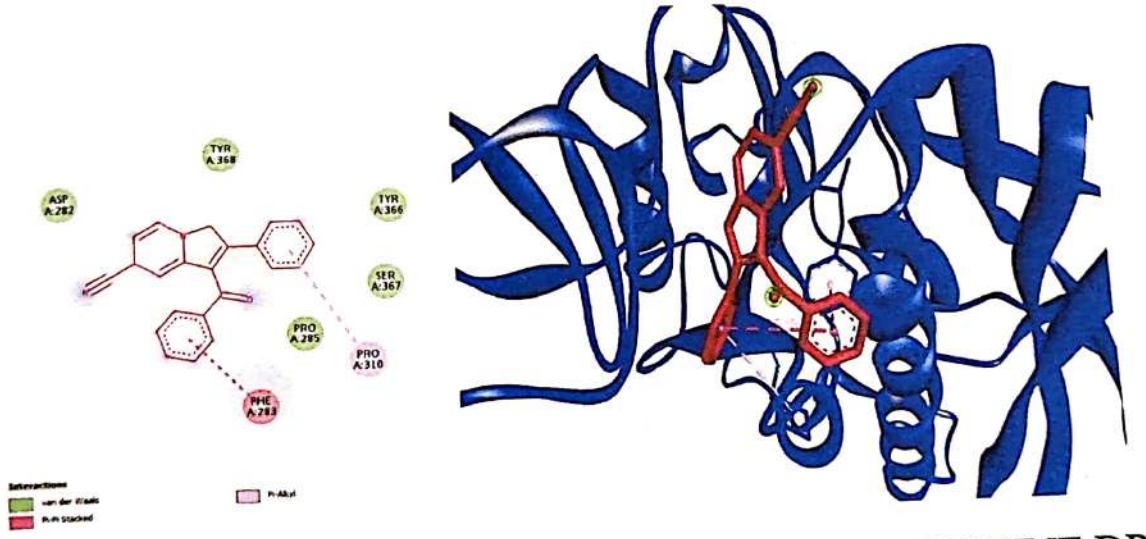


Figure 5: 2D AND 3D STRUCTURE OF 3CL4 -INDOLIZINE DRUG

1-Benzoyl-2-Phenylindolizine-7-Carbonitrile shows binding energy of -6.8 kcal/mol it makes pi-alkyl bonding with amino acid PRO310 along with bond length 5.43. It also shows bonding viz. pi-pi stacking with amino acid PHE283 with bond length 5.19 shown in figure 5.

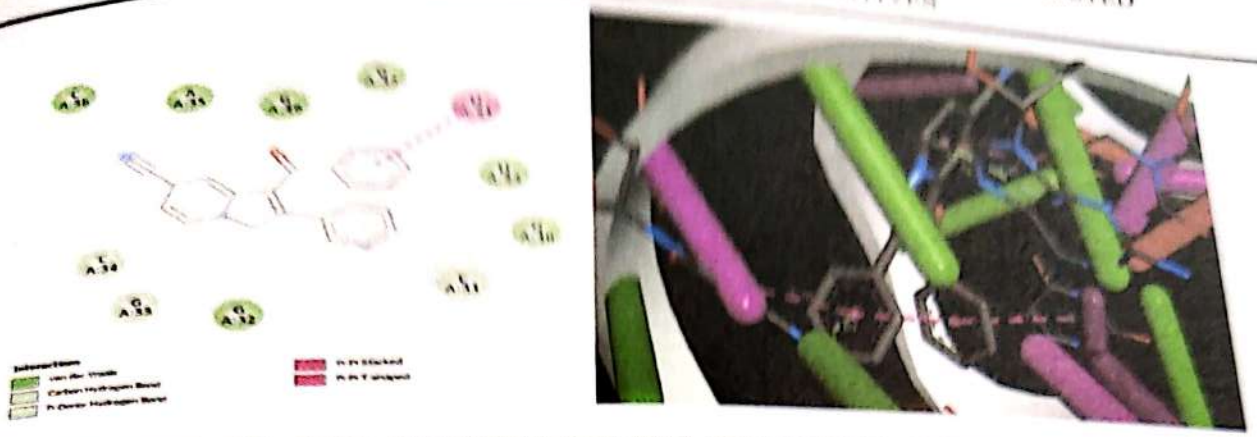

FIGURE 14: 2D AND 3D STRUCTURE OF 7MKY -INDOLIZINE DRUG

ADME and toxicity studies:-

The pharmacokinetic and toxicological profile of the ligand is very important for the alteration of a molecule into a potent drug. In this study, we perform ADMET studies using SwissADME and pkCSM servers. The absorption potential and the lipophilicity of the molecule are characterized by the partition coefficient (log P) and the total polar surface area (TPSA), respectively. The drug molecule penetrates the cell membrane easily as long as the TPSA is > 140 Å. The ideal Log P value of drugs are playing a crucial role for the specific drug target. The Log P-value for oral and sublingual absorption is 1.35 – 1.80; sublingual absorption, > 5 and central nervous system, 2. The penetration of drug to blood brain barrier (BBB) value ranges between -3.0 and 1.2, and for aqueous solubility of ligands ranges values in between -6.5 to 0.5. The P-glycoprotein substrate is chargeable for the efflux of a substrate from inside to outside the cell, and its inhibition reasons drug resistance. In addition, the human intestinal absorption (HIA, %) of ligands is characterized in low, medium and high value ranges of 0 to 29%, 30 to 79% and 80 to 100%, respectively.

Arabian Journal of Chemistry (2020) 13, 6009–6039

King Saud University

Arabian Journal of Chemistry

www.ksu.edu.sa
www.sciencedirect.com

REVIEW ARTICLE

# Starburst pamam dendrimers: Synthetic approaches, surface modifications, and biomedical applications

**Rohini Kharwade** [a,1], **Sachin More** [a,2], **Amol Warokar** [a,3], **Pratibha Agrawal** [b,4], **Nilesh Mahajan** [a,*]

[a] *Dadasaheb Balpande College of Pharmacy, Besa, Rashtrasant Tukadoji Maharaj Nagpur University, Nagpur, MS, India*
[b] *Laxminarayan Institute of Technology, Rashtrasant Tukadoji Maharaj Nagpur University, Nagpur, MS, India*

Received 4 March 2020; accepted 2 May 2020
Available online 13 May 2020

**KEYWORDS**

PAMAM;
Supramolecular dendrimer;
Synthesis;
Biomedical application;
Nanotherapeutics;
Cytotoxicity

**Abstract** Dendrimers are having novel three dimensional, synthetic hyperbranched, nano-polymeric structure. Among all of the dendrimers, Poly-amidoamine (PAMAM) dendrimer are used enormously applying materials in supramolecular chemistry. This review described the structure, characteristic, synthesis, toxicity, and surface modification of PAMAM dendrimer. Various strategies in supramolecular chemistry of PAMAM for synthesizing it at commercial and laboratory scales along with their limitations and applications has also discussed. When compared to other nano polymers, the characteristics of supramolecular PAMAM dendrimers in nanopolymer science has shown significant achievement in transporting drugs for molecular targeted therapy, particularly in host–guest reaction. It also finds its applications in gene transfer devices and imaging

* Corresponding author at: Department of Pharmaceutics, Dadasaheb Balpande College of Pharmacy, Rashtrasant Tukadoji Maharaj Nagpur University, Nagpur, MS 440037, India.
E-mail address: nmmahajan78@gmail.com (N. Mahajan).
[1] Department of Pharmaceutics, Dadasaheb Balpande College of Pharmacy, Rashtrasant Tukadoji Maharaj Nagpur University, Nagpur, MS 440037, India.
[2] Department of Pharmacology, Dadasaheb Balpande College of Pharmacy, Rashtrasant Tukadoji Maharaj Nagpur University, Nagpur, MS 440037, India.
[3] Department of Chemistry, Dadasaheb Balpande College of Pharmacy, Rashtrasant Tukadoji Maharaj Nagpur University, Nagpur, MS 440037, India
[4] Department of Applied Chemistry, Laxminarayan Institute of Technology, Rashtrasant Tukadoji Maharaj Nagpur University, Nagpur, MS 440037, India.

Peer review under responsibility of King Saud University.

Production and hosting by Elsevier

https://doi.org/10.1016/j.arabjc.2020.05.002

**Table 1** Different types of dendrimers with its structural specificity and applications.

| Sr. No. | Types of dendrimers | Synthesis/First reported by | Structural specificity | Applications | Structure | References |
|---|---|---|---|---|---|---|
| 1 | Polyamidoamine dendrimers (PAMAM) | Divergent method/ Tomalia et al. | Spheroidal or ellipsoidal with the presence of several peripheral functional groups and internal cavities | Diagnostic agent. Targeting drug delivery and gene therapy. | 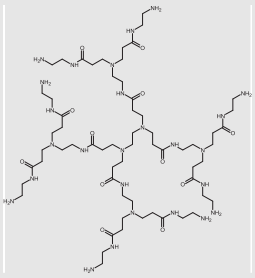 | Naylor, 1989; Negar and Rouhollah, 2013; Pagé and Roy, 1997; Tomalia et al.,1985 |
| 2 | Chiral dendrimers | Convergent method/ Diederich et al. | Peripheral primary amines groups and tertiary propylene amines as a core. Chirality based on the constitutionally different but chemically analogous branches. | Enantioselective catalysis and molecular recognition process. | 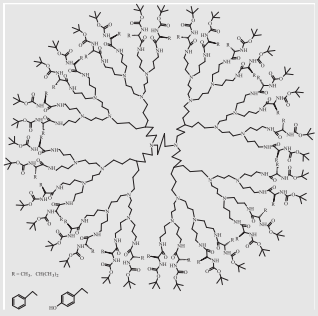 | Ritźen and Frejd, 1999; Smith and Diederich, 1998 |
| 3 | Liquid crystalline dendrimers | Divergent or convergent method /Virgil percec et al. | Mesogenic liquid crystalline monomers or thermotropic liquid crystalline phases which are rod-like (calamitic) or disk-like (Discotic) molecules. | Use for specific physical properties. | 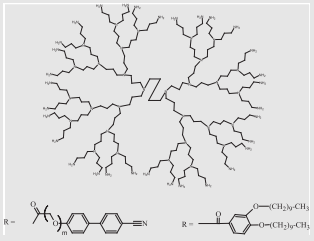 | Cheng et al., 2015a, 2015b; Guillon and Deschenaux, 2002; Percec et al., 1992; Smith and Diederich, 1998 |
| 4 | Polypropylene ether imine dendrimers (PPI) | Divergent method/ Newkome et al. | Amino butane core with primary amines as functional end groups. | Antimicrobial and solubility enhancement agent. | 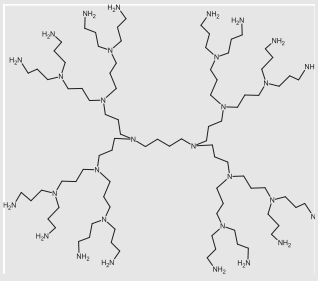 | Gillies et al., 2005; Inoue, 2000; Kaur et al., 2016; Newkome et al., 1986 |
| 5 | Tecto dendrimers | Divergent method/Tam et al. | Fluorescein core (thermotropic agent) and folate as a functionally active peripheral moiety. | Used for Multidrug delivery, gene therapy, and environmental remediation. | 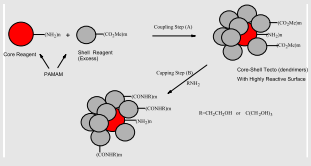 | Schilrreff et al., 2012; Tam and Lu, 1995; Welch and Welch, 2009 |
| 6 | Peptide dendrimers | Convergent method/Sadler et al. | Amino acid as peripheral and interior unit. | Used for the diagnostic purpose, vaccine delivery, protein replacement, Chemotherapeutic agent and gene therapy. | 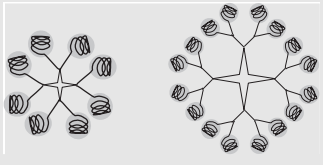 | Ammonium, 1995; Backbone, 1990; Sadler and Tam, 2002 |

**Table 1** (*continued*)

| Sr. No. | Types of dendrimers | Synthesis/First reported by | Structural specificity | Applications | Structure | References |
|---|---|---|---|---|---|---|
| 7 | Carbosilane dendrimers | Divergent and convergent method/ Bermejo et al. | Two different cores 1,3,5-$(HO)_3C_6H_3$ and $Si(C_3H_5)_4$ having carboxylate and sulfonate as an end functional groups. | Potential application in catalysis, host–guest chemistry, novel polymer topology. | 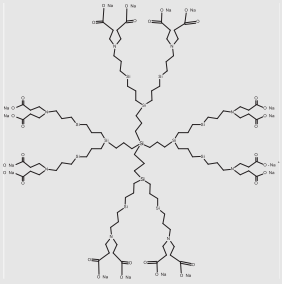 | Bermejo et al., 2007; Kesharwani et al., 2014 |
| 8 | Glycodendrimers | Divergent and convergent method/ Benjamin Davis et al. | Glycodendrimers include sugar moieties such as mannose, glucose, galactose, and disaccharide. | In biotechnology and material science. | 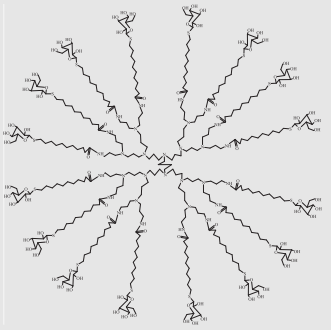 | Benjamin, 2002; Roy and Baek, 2002; |
| 9 | Triazine dendrimers | Convergent method (cycloaddition reaction or triazene substitution)/ Astruc et al. | The core is containing triazine trichloride and other triazine based compounds. | Used in the synthesis of simazine herbicide also applied in non-viral gene delivery. | 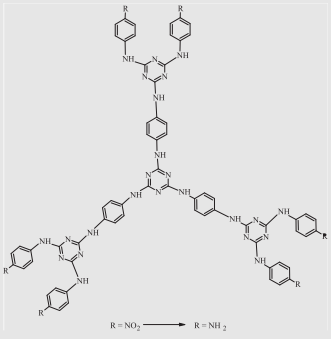 | Astruc et al., 2012; Steffensen et al., 2006 |
| 10 | Hybrid dendrimer | A Divergent method (Diels-Alder cycloaddition) by Roovers et al. | These are hybrids of dendritic and linear polymers. Composed of elastic carbosilane core and rigid aromatic shell. | As drug carriers. | 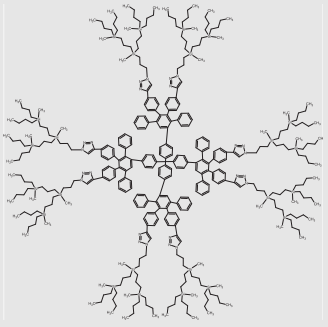 | Kesharwani et al., 2014; Roovers and Comanita, 1999 |
| 11 | PAMAMOS (Poly amidoamine Organosilicon Dendrimers) | Divergent method/Peter Dvornic et al. | PAMAM as an interior and hydrophobic organosilicon as a peripheral moiety. | Use for drug conjugate and nanocarrier. | 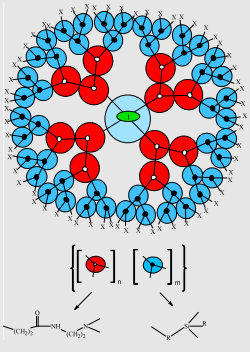 | Dvornic, 2006; Tomalia, 1993; Torchilin, 2006 |

(*continued on next page*)

**Table 1** (*continued*)

| Sr. No. | Types of dendrimers | Synthesis/First reported by | Structural specificity | Applications | Structure | References |
|---|---|---|---|---|---|---|
| 12 | Multiple antigen peptide dendrimers | Convergent and Divergent method/Tam et al. | Dendron like molecular configuration based on a polylysine framework. | Improved efficiency of antibiotics and antimicrobial molecules. | 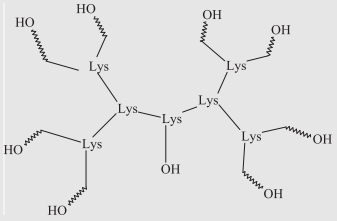 | Joshi et al., 2013; Tam and Lu, 1995 |
| 13 | Frechet-type dendrimers | Convergent method/ Hawker and Frechet et al. | Structural framework based polybenzyl ether with Carboxylic acid group act as a functionally active peripheral moiety. | Pharmaceutically active compound, imaging agent, radioligand and targetting molecule. | 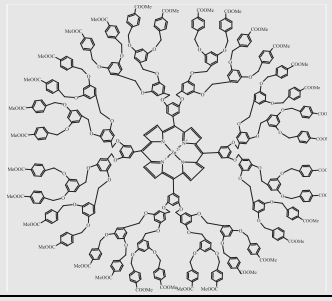 | Hawker and Fréchet, 1990; Ihre et al., 2002 |

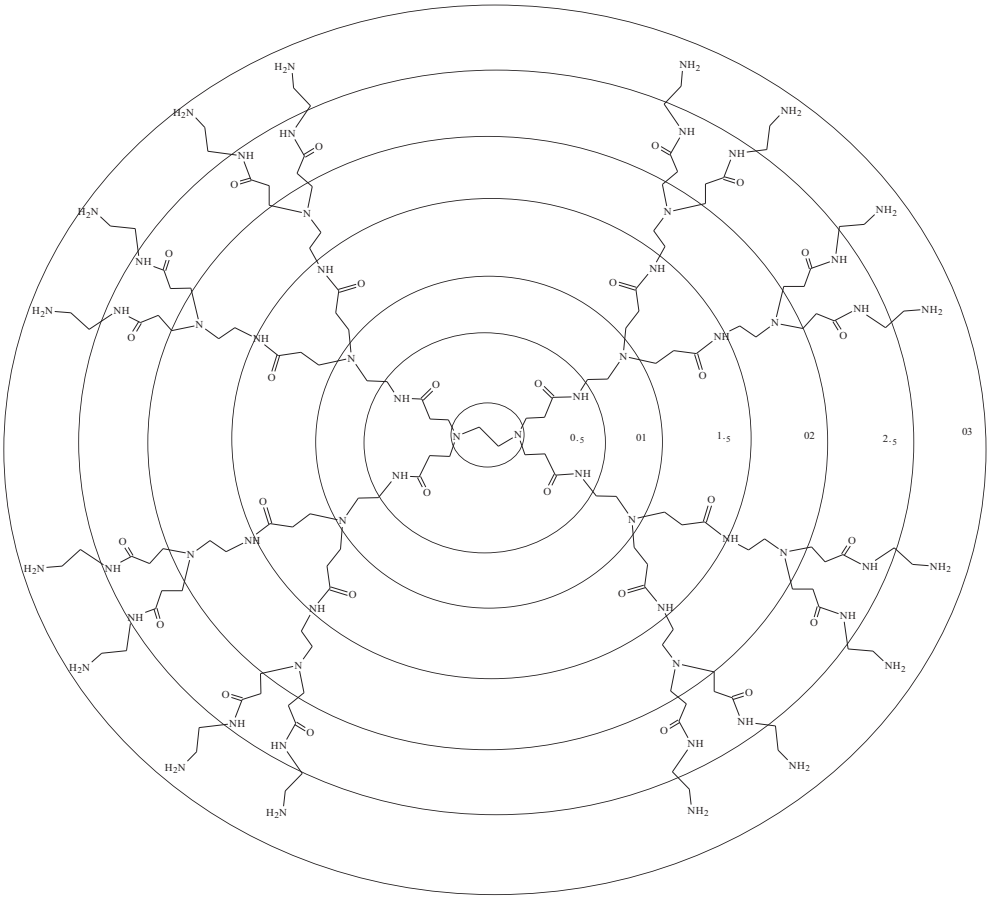

**Fig. 1** Structure of PAMAM dendrimer with the generation's number and the peripheral end groups.

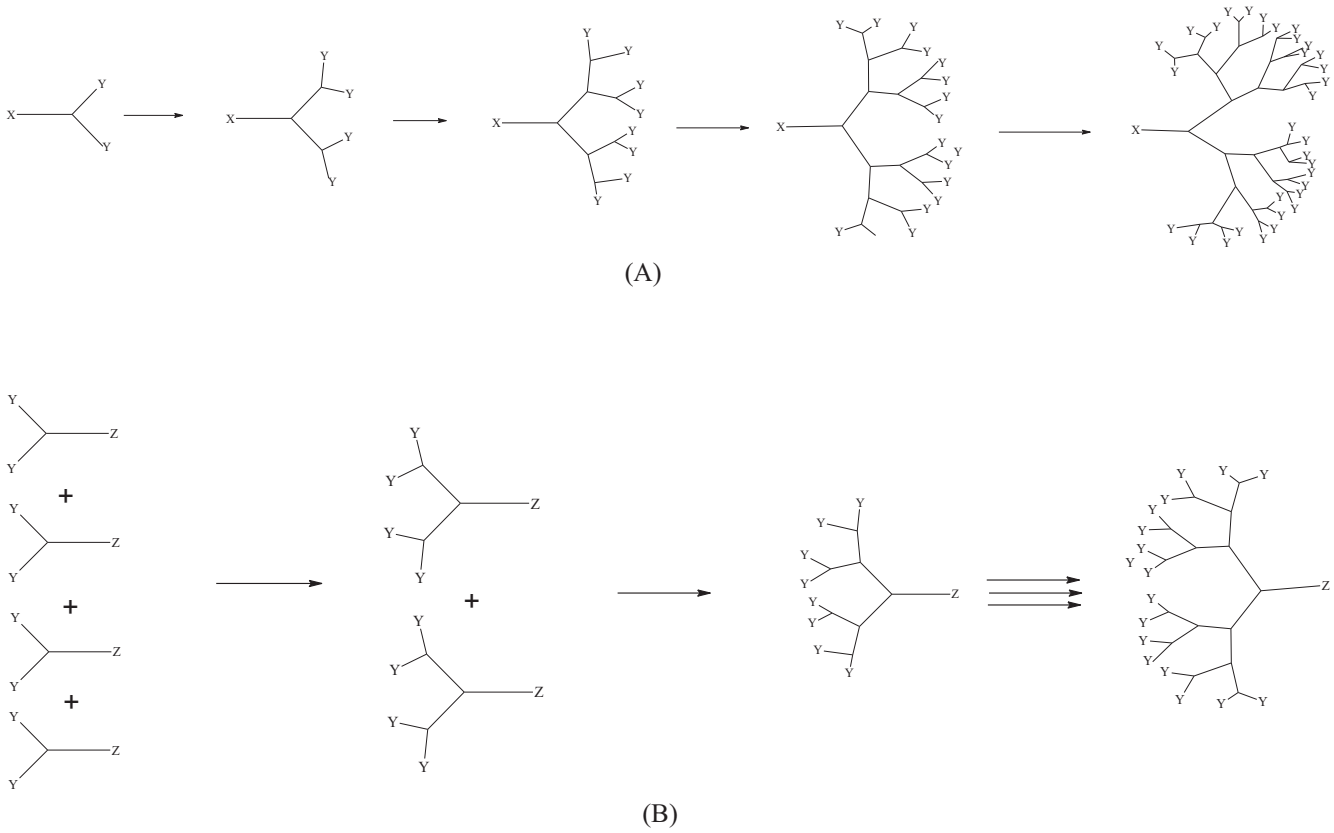

**Scheme 2** Diagramatic illustration of divergent (A) and convergent (B) synthetic approach for dendrimers.

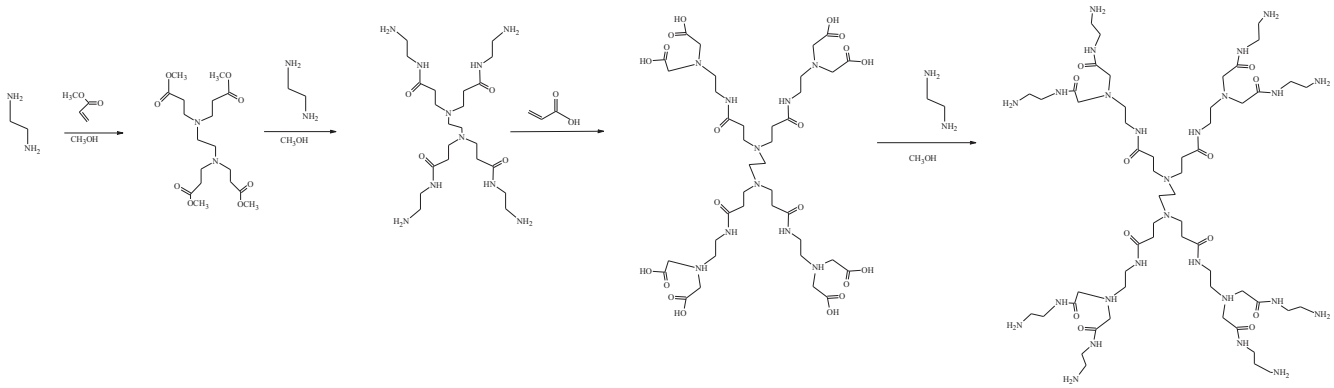

**Scheme 3** Divergent approach for synthesizing PAMAM dendrimer (Labieniec-Watala and Watala, 2015).

urine and feces twice over seven days as compared to polycationic dendrimer (Nigavekar et al., 2004). Nigavekar and his coworkers compared PAMAM G5 dendrimer with surface modified acetylated PAMAM dendrimer for biodistribution. They used B16 melanoma cell line and DU145 human prostate cancer cell line. They observed that tissue deposition of polycationic PAMAM is better as compared to the neutral surface charge (Nigavekar et al., 2004). From that observation, they conclude that neutralization of surface charge of PAMAM dendrimers is required to utilize it as a systemic biomedical delivery device. Drugs interact with the PAMAM dendrimer molecule and encapsulate into the interior cavities by electrostatic interactions or by conjugation with the end groups.

Sadekar et al. compared the effect of the multiple branched PAMAM dendrimers and linear N-(2-hydroxypropyl)metha crylamide (HPMA) copolymers on tumor-bearing mice. They identified the effect of molecular weight and hydrodynamic size of PAMAM and HPMA on biodistribution using compartmental pharmacokinetic analysis. They observed that hydroxyl-terminated PAMAM dendrimers have higher tumor

was able to lower intracellular reactive oxygen species and to reduce the level of cleaved caspase-3 at low concentration (Pojo et al., 2013). Recently Gao et al. reported the use of G4 PAMAM to remineralize human teeth to treat dentine hypersensitivity. They demonstrated that PAMAM created precipitates on the surface and within the dentinal tubules with a strong ability to resist acid and showed great potential in the treatment of dentine hypersensitivity (Gao et al., 2017).

## 8. Conclusion

PAMAM dendrimers are hyperbranched organic molecules with distinguished characteristics from all other traditional linear polymers like size, shape, monodispersity, surface charge and peripheral functional group. For achieving these unique characteristics optimally, it must be synthesized with consistent quality and purity. Various approaches for synthesizing PAMAM dendrimers have been available, including divergent, convergent along with click chemistry, lego synthesis and hybrid convergent-divergent synthesis. However, preparation of high generation and defect-free PAMAM dendrimers on a large scale remains challenging because the purification processes are complicated and require the appropriate handling of energy parameters.

Due to its physicochemical properties and bio structural similarities, it determined its immense potential in the field pharmaceuticals as well as the bio-medicals. PAMAM dendrimer can improve biological properties such as bioavailability, solubility and specific target selectivity by linking or entrapping bioactive compounds. The peripheral positive charge of PAMAM is responsible for its cytotoxicity which can be overcome by neutralizing charge through PEGylation, acetylation, folate, and peptide conjugation. The structure of PAMAM dendrimers with a wide scope of applications will provides several opportunities for commercialization in the future.

## Declaration of Competing Interest

The research did not receive any scientific grants from funding agencies in the public, commercial, or not for profit sectors.

## References

Abbasi, E., Aval, S.F., Akbarzadeh, A., Msilani, M., Nasrabadi, H. T., 2014. Dendrimers: synthesis, applications, and properties. Nanoscale Res. Lett. 9, 1–10.

Abedi-Gaballu, F., Dehghan, G., Ghaffari, M., Yekta, R., Abbaspour-Ravasjani, S., Baradaran, B., Dolatabadi, J.E.N., Hamblin, M.R., 2018. PAMAM dendrimers as efficient drug and gene delivery nanosystems for cancer therapy. Appl. Mater. Today 12, 177–190. https://doi.org/10.1016/j.apmt.2018.05.002.

Agashe, H.B., Dutta, T., Garg, M., Jain, N.K., 2006. Investigations on the toxicological profile of functionalized fifth-generation poly (propylene imine) dendrimer. J. Pharm. Pharmacol. 58, 1491–1498. https://doi.org/10.1211/jpp.58.11.0010.

Al-Jamal, K.T., Ramaswamy, C., Florence, A.T., 2005. Supramolecular structures from dendrons and dendrimers. Adv. Drug Deliv. Rev. 57, 2238–2270. https://doi.org/10.1016/j.addr.2005.09.015.

Alper, J., 1991. Rising chemical "stars" could play many roles. Science 251 (5001), 1562–1564. https://doi.org/10.1126/science:2011736.

Ammonium, C., 1995. F-1; 578, 578–581.

Astruc, D., Chardac, F., 2001. Dendritic catalysts and dendrimers in catalysis. Chem. Rev. 101, 2991–3023. https://doi.org/10.1021/cr010323t.

Astruc, D., Liang, L., Rapakousiou, A., Ruiz, J., 2012. Click dendrimers and triazole-related aspects: Catalysts, mechanism, synthesis, and functions. A bridge between dendritic architectures and nanomaterials. Acc. Chem. Res. 45, 630–640. https://doi.org/10.1021/ar200235m.

Backbone, P.L., 1990. X (x * 425–430).

Bahadoran, A., Ebrahimi, M., Yeap, S.K., Safi, N., Moeini, H., Hair-Bejo, M., Hussein, M.Z., Omar, A.R., 2017. Induction of a robust immune response against avian influenza virus following transdermal inoculation with H5-DNA vaccine formulated in modified dendrimer-based delivery system in mouse model. Int. J. Nanomed. 12, 8573–8585. https://doi.org/10.2147/IJN.S139126.

Bai, S.C., Thomas, F.A., 2007. Dendrimer as a carrier for pulmonary delivery of enoxaparin, a low – molecular weight heparin. J. Pharm. Sci. 96, 2090–2106. https://doi.org/10.1002/jps.20849.

Barrett, T.G., Ravizzini, P.L., Choyke, H.K., 2017. Dendrimers in medical science. Dendrimers Med. Sci., 1–221 https://doi.org/10.1201/9781315366005.

Benjamin, D., 2002. Synthesis and use of glycodendrimer reagents related application data.

Bermejo, J.F., Ortega, P., Chonco, L., Eritja, R., Samaniego, R., Müllner, M., De Jesus, E., De La Mata, F.J., Flores, J.C., Gomez, R., Munoz-Fernandez, A., 2007. Water-soluble carbosilane dendrimers: Synthesis biocompatibility and complexation with oligonucleotides; evaluation for medical applications. Chem. – A Eur. J. 13, 483–495. https://doi.org/10.1002/chem.200600594.

Bertero, A., Boni, A., Gemmi, M., Gagliardi, M., Bifone, A., Bardi, G., 2014. Surface functionalisation regulates polyamidoamine dendrimer toxicity on blood-brain barrier cells and the modulation of key inflammatory receptors on microglia. Nanotoxicology 8, 158–168. https://doi.org/10.3109/17435390.2013.765054.

Bhadra, D., Bhadra, S., Jain, N.K., 2005. Pegylated lysine based copolymeric dendritic micelles for solubilization and delivery of artemether. J. Pharm. Pharm. Sci. 8, 467–482.

Bosman, A.W., Janssen, H.M., Meijer, E.W., 1999. About dendrimers: structure, physical properties, and applications. Chem. Rev. 99, 1665–1688. https://doi.org/10.1021/cr970069y.

Brouwer, A.J., Mulders, S.J.E., Liskamp, R.M.J., 2001. Convergent synthesis and diversity of amino acid based dendrimers. Eur. J. Org. Chem. 25, 1903–1915. https://doi.org/10.1002/1099-0690(200105)2001:10<1903::AID-EJOC1903>3.0.CO;2-W.

Bugno, J., Hsu, H.J., Hong, S., 2015. Recent advances in targeted drug delivery approaches using dendritic polymers. Biomater. Sci. 3, 1025–1034. https://doi.org/10.1039/c4bm00351a.

Cakara, D., Kleimann, J., Borkovec, M., 2003. Microscopic protonation equilibria of poly(amidoamine) dendrimers from macroscopic titrations. Macromolecules 36, 4201–4207. https://doi.org/10.1021/ma0300241.

Caminade, A.M., Laurent, R., Majoral, J.P., 2005. Characterization of dendrimers. Adv. Drug Deliv. Rev. 57, 2130–2146. https://doi.org/10.1016/j.addr.2005.09.011.

Cancino, J., Paino, I.M.M., Micocci, K.C., Selistre-de-Araujo, H.S., Zucolotto, V., 2013. In vitro nanotoxicity of single-walled carbon nanotube-dendrimer nanocomplexes against murine myoblast cells. Toxicol. Lett. 219, 18–25. https://doi.org/10.1016/j.toxlet.2013.02.009.

Chauhan, A.S., 2018. Dendrimers for drug delivery. Molecules 23. https://doi.org/10.3390/molecules23040938.

Chauhan, A.S., Jain, N.K., Diwan, P.V., Khopade, A.J., 2004. Solubility enhancement of indomethacin with poly(amidoamine) dendrimers and targeting to inflammatory regions of arthritic rats. J. Drug Target. 12, 575–583. https://doi.org/10.1080/10611860400010655.

Chauhan, A.S., Sridevi, S., Chalasani, K.B., Jain, A.K., Jain, S.K., Jain, N.K., Diwan, P.V., 2003. Dendrimer-mediated transdermal

# *In Silico Antidiabetic Characterization and ADME Studies of Swertia Chirayita*

*Mini project*

Submitted in partial fulfillment of the

Requirement for the degree of

**Bachelor of pharmacy**

**In**

In the faculty of science & technology,

Rashtrasant Tukdoji Maharaj Nagpur University, Nagpur.

**By**

Miss. Jayshri J. Kumare

Guide

Mr. K. R. Danao

M. Pharm, DDP

Ambe Durga Education Society's

Dadasaheb Balpande college of Pharmacy, Besa

Nagpur -440037

2020-2021

## 2D interaction and 3D interaction of compound with alpha amylase:

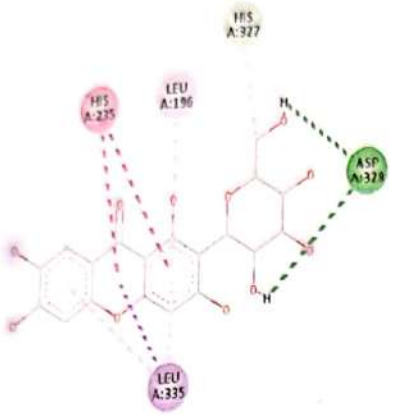


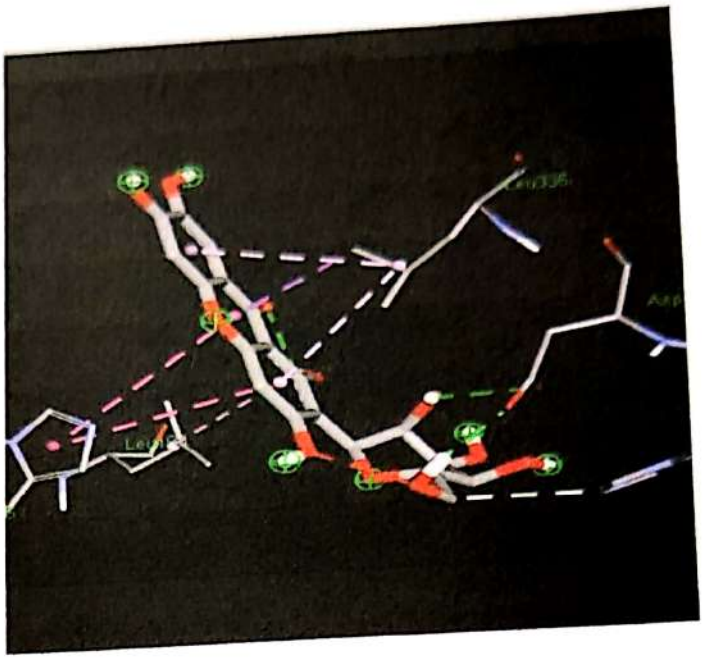

Eg: Mangiferin

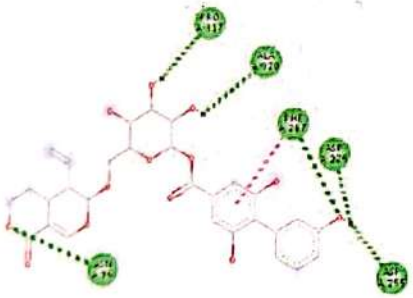

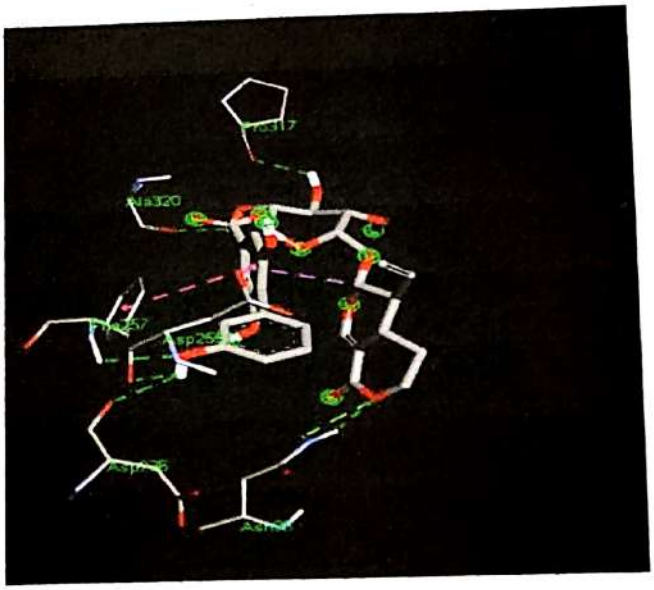

Eg.Amarogentin

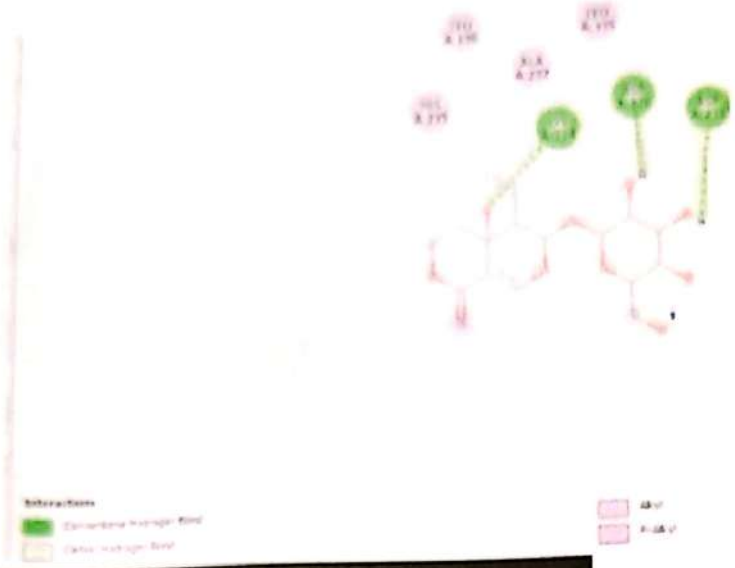

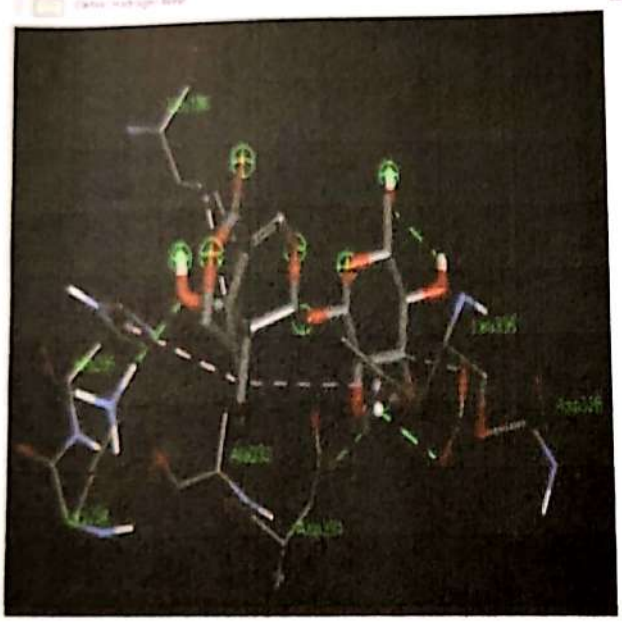

Eg: swertiamarin

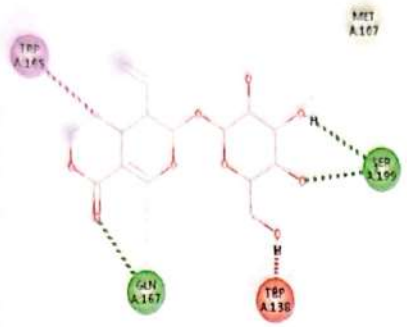

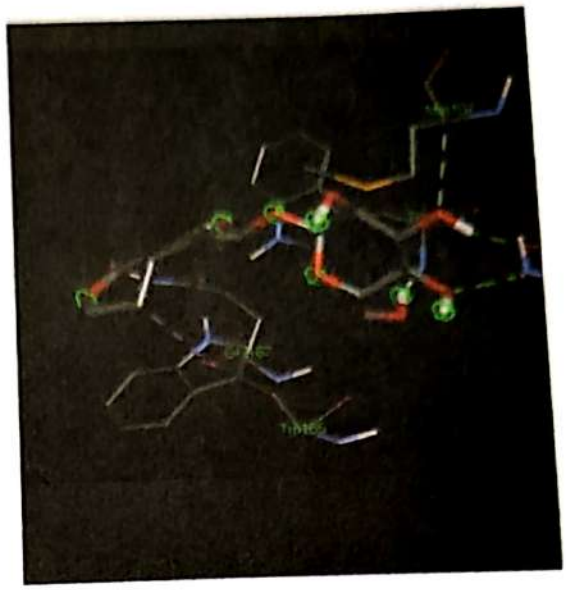

Eg.sweroside

## Ramachandran Plot:

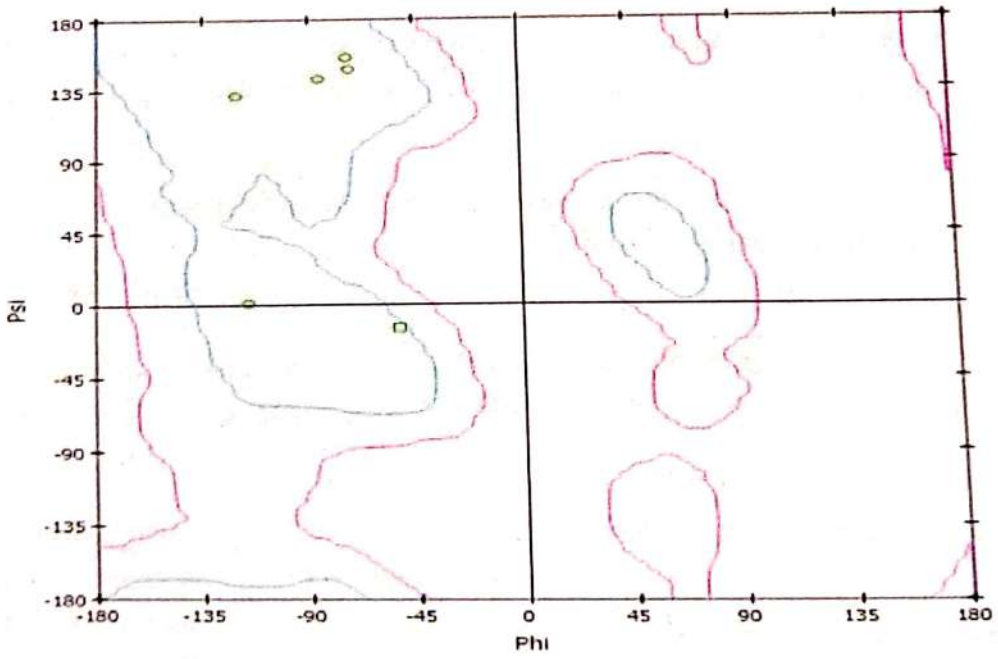


Fig. Ramachandran plot showing allowed region in protein α amylase

# *IN-SILICO* STUDIES OF PHYTOMEDICINES FOR COVID-19: A REVIEW

A PROJECT REPORT

**Submitted to**

Rashtrasant Tukdoji Maharaj Nagpur University,Nagpur

in partial fulfillment of the

requirement for the degree of

**Bachelor of pharmacy**

**In**

**The Faculty of Science and Technology,**

**Submitted By:-**


**Ms. Khushbu Pandhare**

(B.Pharm IV YEAR)


**Guided by :**


**Dr. Deweshri M. Nandurkar**

**Assistant Professor**

**(Department of Pharmaceutical Chemistry)**




**Ambe Durga Education Society's**

**Dadasaheb Balpande College of Pharmacy, BesaNagpur-440037**


**2021-2022**

| | | | | | |
|---|---|---|---|---|---|
| 16 | Dalchini  | *Cinnamomum verum* | ✔ | Antiviral agent | Camphoratin D[40] 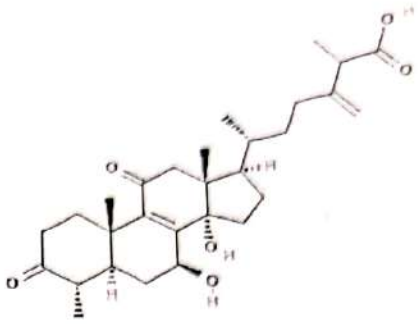 |
| 17 | Aloe-Vera  | *Aloe barbadensis miller* | ✔ | Antioxidant agent | Feralolide[41] 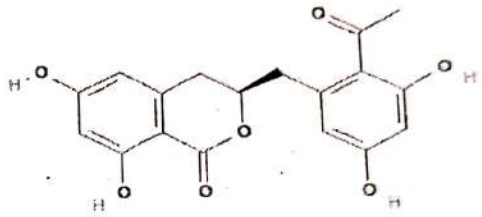 |
| 18 | Fingered citron  | *Citrus medica* | ✔ | Antioxidant agent | Rhoifolin [42] 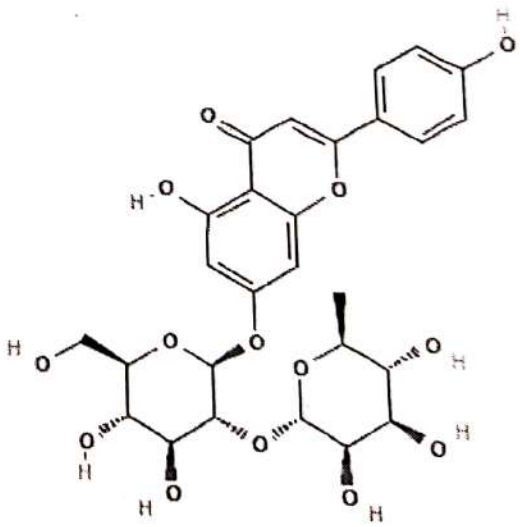 |

# DESIGN OF 2-AMINO-4-CHLROPHENOL SCHIFF BASE METAL COMPLEX FOR COVID-19 DISEASE: AN IN-SILICO APPROACH

## A PROJECT REPORT

Submitted to

Rashtrasant Tukadoji Maharaj Nagpur University, Nagpur

in partial fulfillment of the

Requirement for the degree of

**Bachelor of Pharmacy**

**In**

**The Faculty of Science & Technology.**

Submitted By

**Mr. Mayur D. Mahajan**
**Mr. Jatin A. Nagrale**
**(B. pharm final year)**

**Guide**

**Mrs. Ruchi Shivhare**

**Assistant professor**



**Ambe Durga Education Society's**

**Dadasaheb Balpande College of Pharmacy**

Near swami samarth dham mandir, Besa Nagpur – 440037

2021-2022

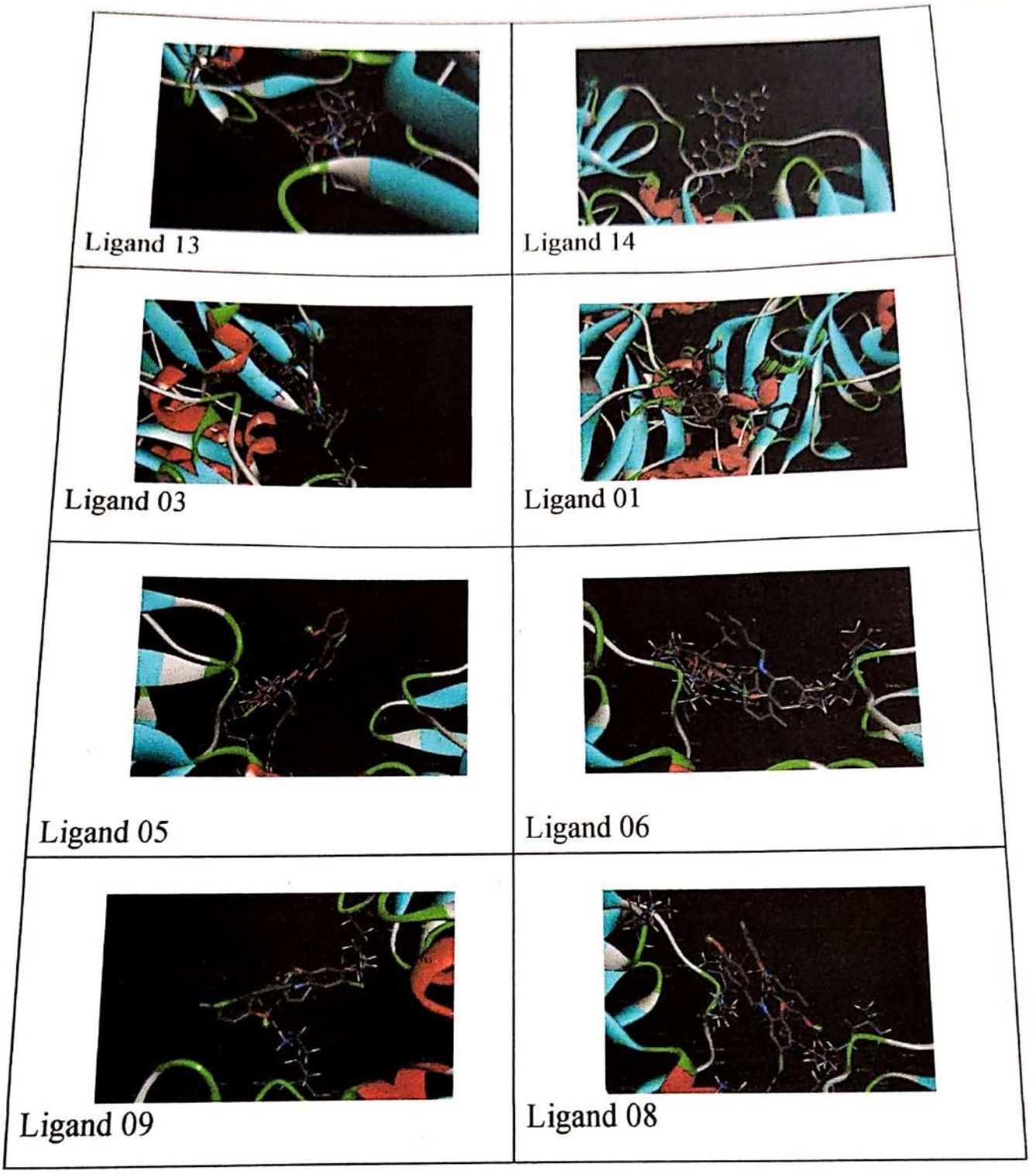


**Fig2**; Protein ligand interactions

## Literature Review

# Design, Synthesis, Pharmacological evaluation and *In-silico* study of new 2-oxo-4-substituted aryl-azetidine Benzotriazole derivatives

Submitted in partial fulfillment of the

requirement for the degree of

**Bachelor of Pharmacy**

In the Faculty of Science & Technology,

Rashtrasant Tukadoji Maharaj Nagpur University, Nagpur.

**By**


Miss. Priyanka. Yadav

**Guide**

Mrs. Vijayashri. Rokde




**Ambe Durga Education Society's**

**Dadasaheb Balpande College of Pharmacy, Besa,**

**Nagpur – 440037**


**2021-2022**

**Docking result: -**

## 4- Hydroxy derivative

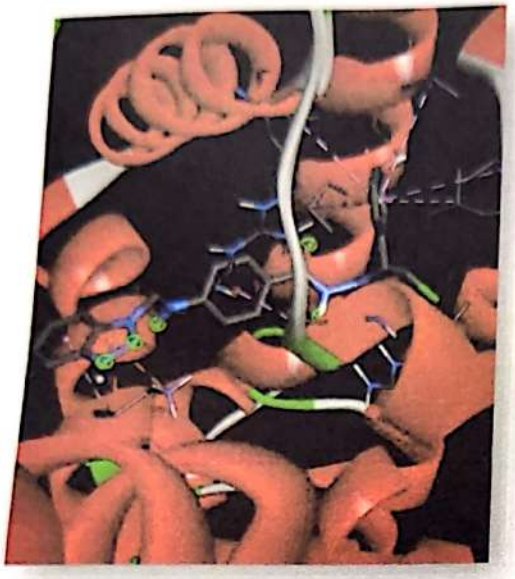

3D structure

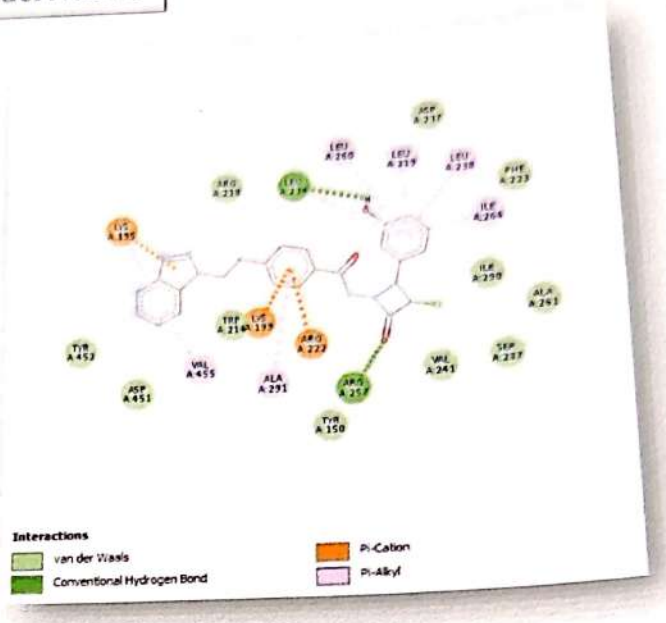


2D structure

## 2-Nitro derivative

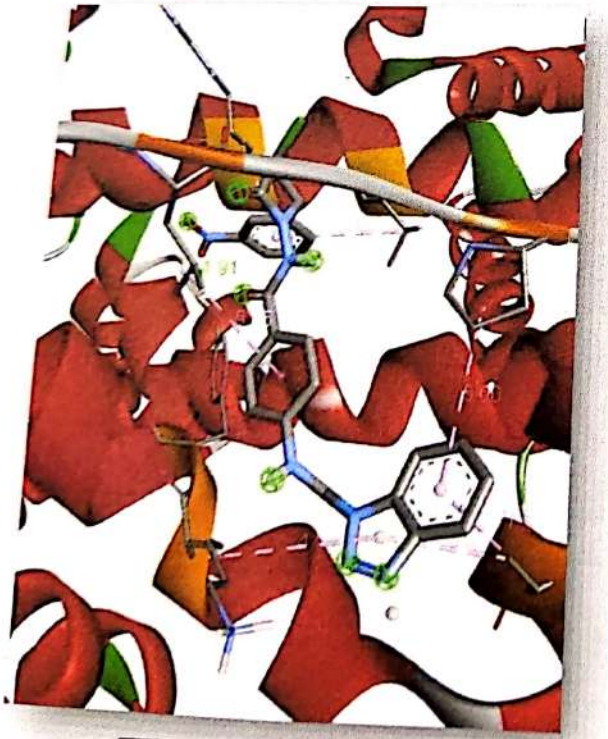

3D structure

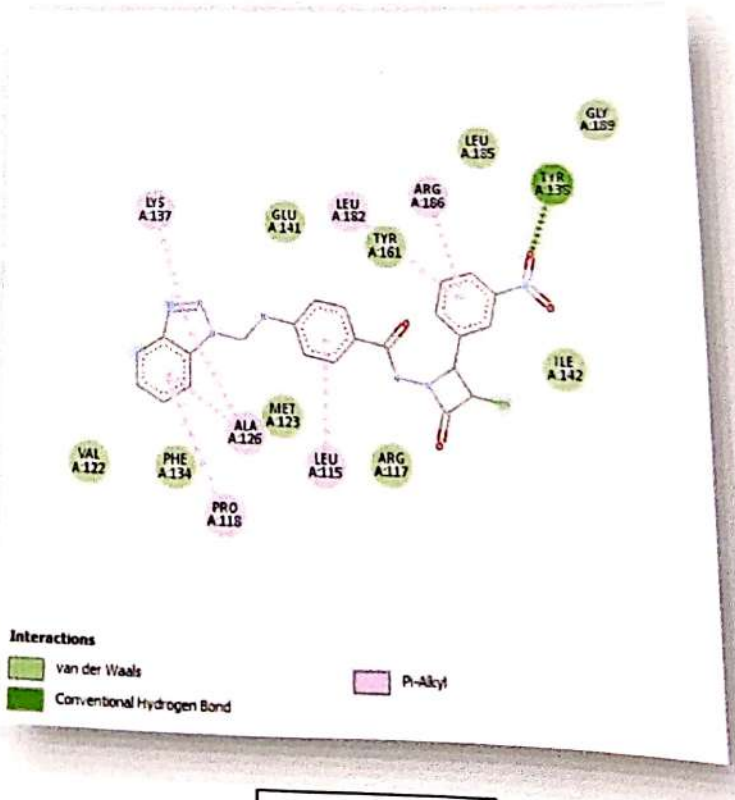


2D structure

**Docking result: -**

| Sr.No. | Ligand | Binding Affinity |
|---|---|---|
| 1. | 4- Hydroxy benzaldehyde | -11.2 |
| 2. | 2- Nitro benzaldehyde | -10.1 |
| 3. | 4- Nitro benzaldehyde | -9.8 |
| 4. | p- chloro benzaldehyde | -10.1 |
| 5. | Anisaaldehyde | -10 |
| 6. | Benzaldehyde | -11 |
| 7. | p- Amino dimethyl benzaldehyde | -10.4 |
| 8. | 3- Nitro benzaldehyde | -10.1 |
| 9. | 3- Hydroxy 4- methoxy benzaldehyde | -10.2 |
| 10. | 4- Methoxy benzaldehyde | -10.1 |
| 11. | 2,3- Dimethyl benzaldehyde | -10.3 |
| 12. | 2- Bromo benzaldehyde | -10.4 |
| 13. | N-(3-ethylphenyl) formamide | -10.2 |
| 14. | 4- Methyl benzaldehyde | -10.2 |
| 15. | 2- Hydroxy benzaldehyde | -10.4 |
| 16. | 3,4,5- Trimethoxy benzaldehyde | -8.9 |

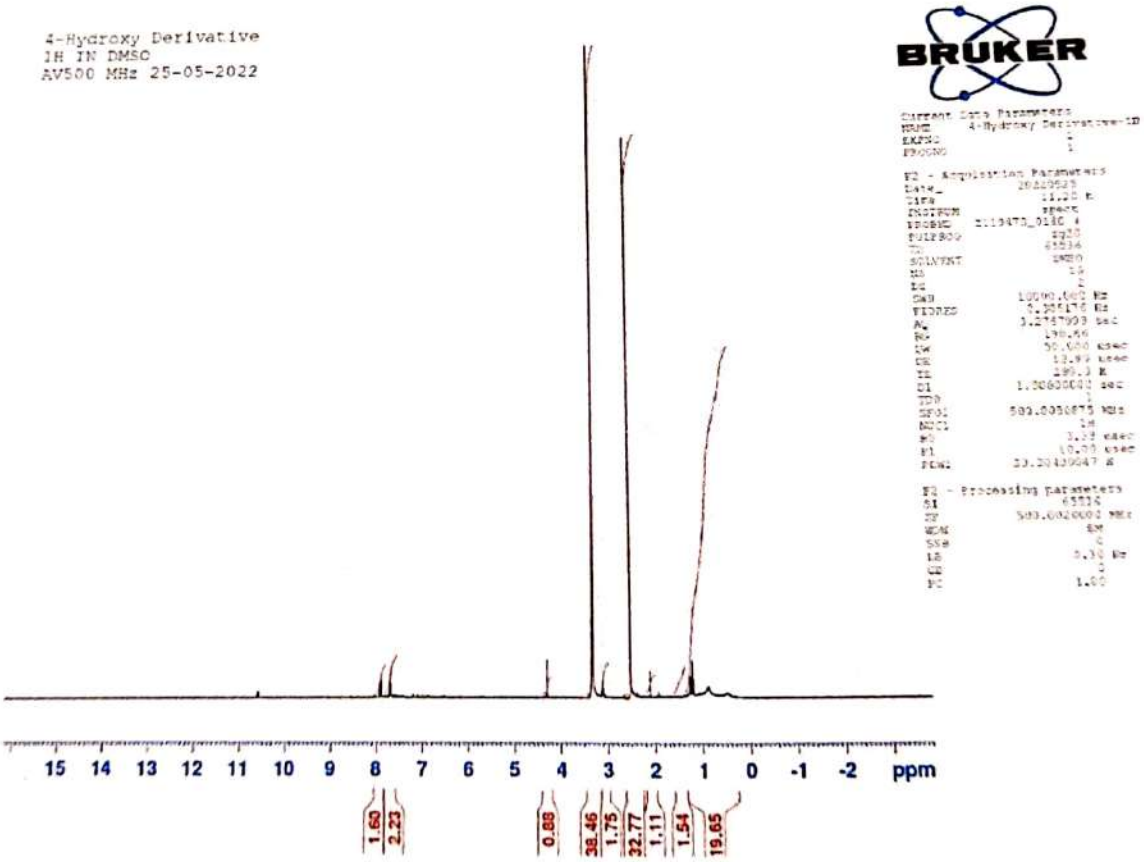


**4- Hydroxy derivative**

383

# In Silico Study of Abutilon Indicum for Hypoglycaemic activity

A PROJECT REPORT

Submitted in partial fulfillment of the

Requirement for the degree of

**Bachelor of Pharmacy**

In the Faculty of Science & Technology,

Rashtrasant Tukadoji Maharaj Nagpur University, Nagpur.

**By**

**Mr. Rushikesh R. Bobde**

**Guide**

**Mr. Kishor Danao**
**(Asst. Professor, department of Chemistry)**



**Ambe Durga Education Society's**

**Dadasaheb Balpande College of Pharmacy, Besa,**

**Nagpur – 440037**

**2021-2022**

| Phytoconstituents/ADMET | PUBCHEM CID | Molecular weight | Log p | HB Acceptor | HB Donor | Aqueous solubility | Oral Rat Acute Toxicity (LD50) (log mol/kg) |
|---|---|---|---|---|---|---|---|
| Chrysoeriol | 5280666 | 300.26 | 2.18 | 6 | 3 | -3.237 | 2.337 |
| Hinesol | 10878761 | 222.37 | 3.56 | 1 | 1 | -4.429 | 1.683 |
| Luteolin | 5280445 | 286.24 | 1.73 | 6 | 4 | -3.094 | 2.482 |
| Phytol | 5280435 | 296.5 | 6.23 | 0 | 0 | -2.991 | 1.848 |
| Cubenol | 519857 | 222.37 | 3.52 | 1 | 1 | -4.206 | 2.482 |
| Palmitic acid | 985 | 256.42 | 5.20 | 1 | 1 | -5.562 | 3.181 |
| Pinellic acid | 9858729 | 330.5 | 3.11 | 0 | 0 | -1.895 | 1.234 |

Figure 3 : physiochemical and LD 50 dose study of phytoconstituents

Figure 4:- 3D - 7DCH-cherysoeriol

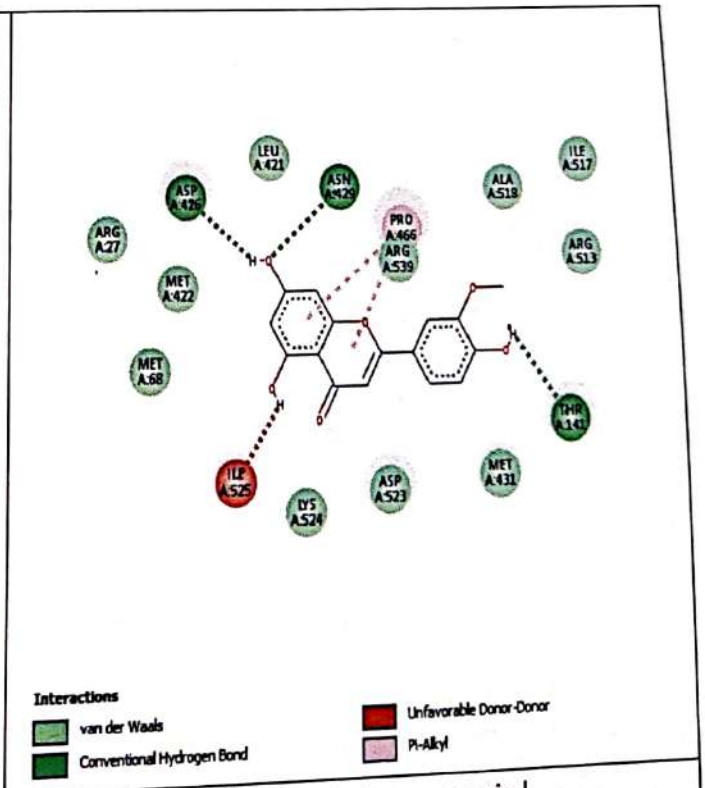


2D - 7DCH-cherysoeriol

Figure 5:- 3D – 7DCH-Cubenol

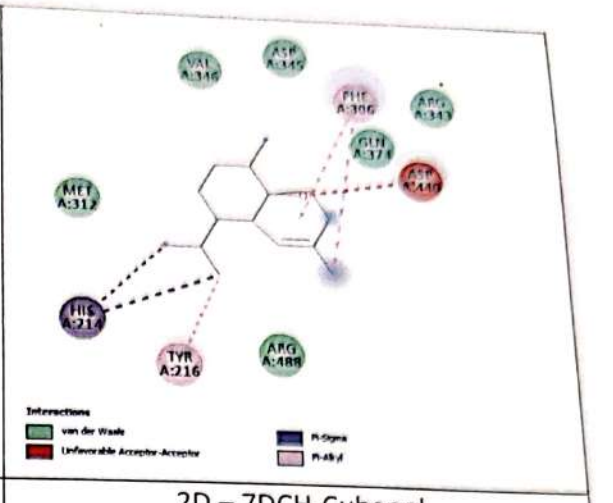


2D – 7DCH-Cubenol

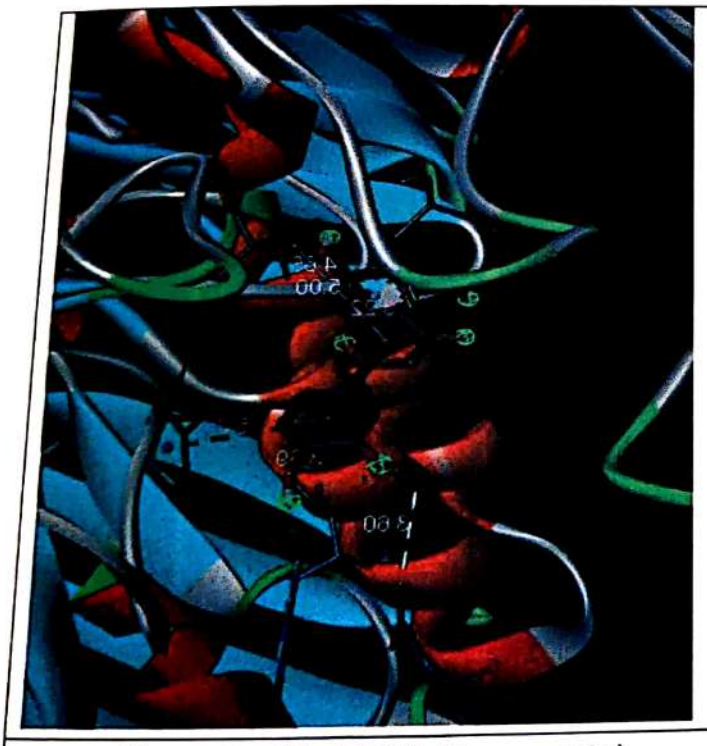

Figure 6:- 3D - 7D9B-Cherysoeriol

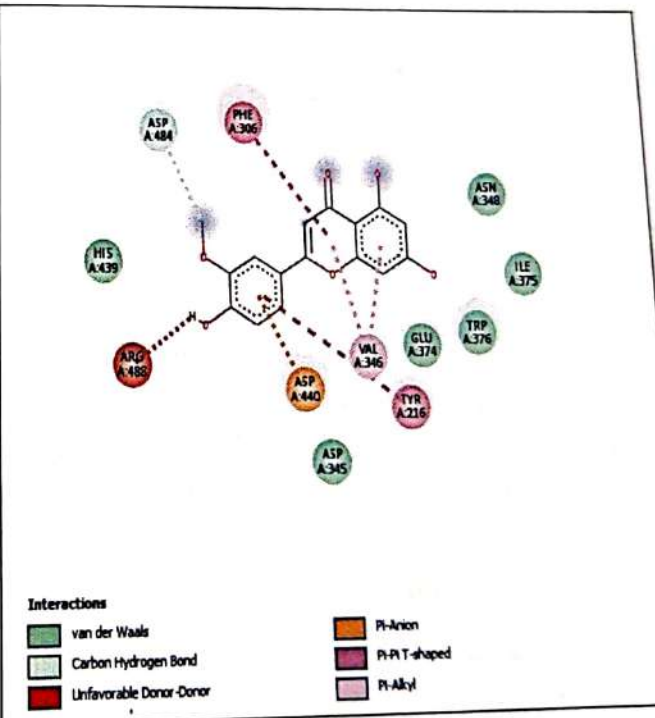


2D - 7D9B-Cherysoeriol

401

# *IN SILICO* INVESTIGATION OF ANILINE SCHIFF BASE TO TARGET THE SARS-COV-2 PROTEINS OF COVID-19

## A PROJECT REPORT

Submitted to

Rashtrasant Tukadoji Maharaj Nagpur University, Nagpur

in partial fulfillment of the

Requirement for the degree of

**Bachelor of Pharmacy**

**In**

**The Faculty of Science & Technology.**

Submitted By


**Mr. Shatayu S. Wasnik**
**(B. pharm IV year)**


**Guide**

**Dr. Deweshri M. Nandurkar**

**Assistant professor**



**Ambe Durga Education Society's**

## Dadasaheb Balpande College of Pharmacy

Near Swami Samarth Dham mandir, Besa Nagpur – 440037

2021-2022

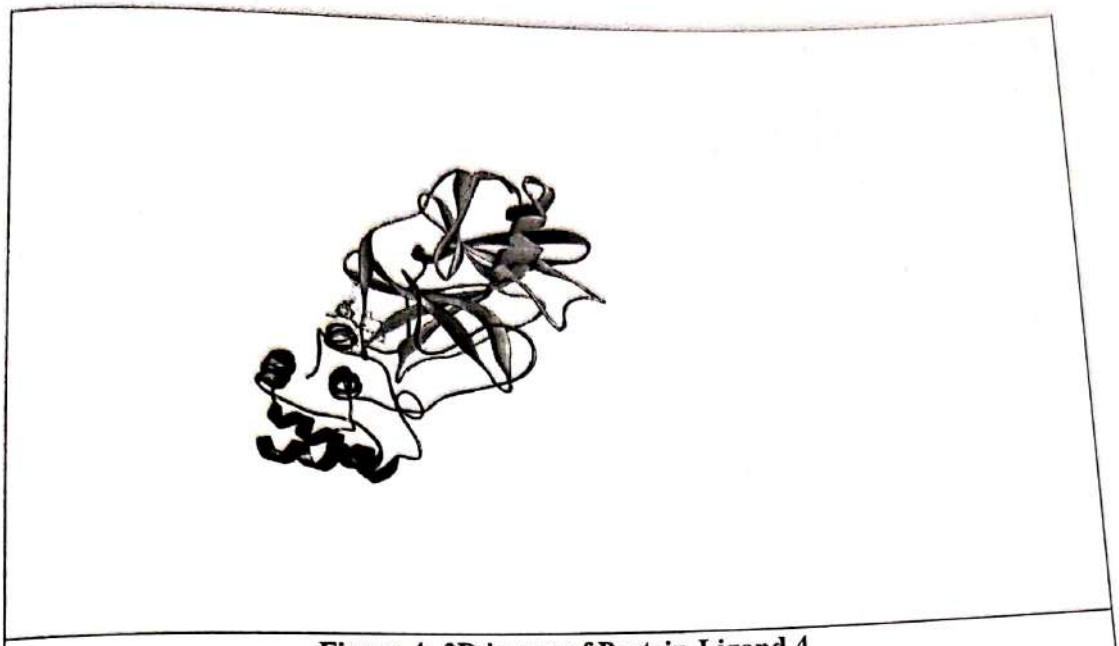

**Figure 4: 3D image of Protein-Ligand 4 interaction**

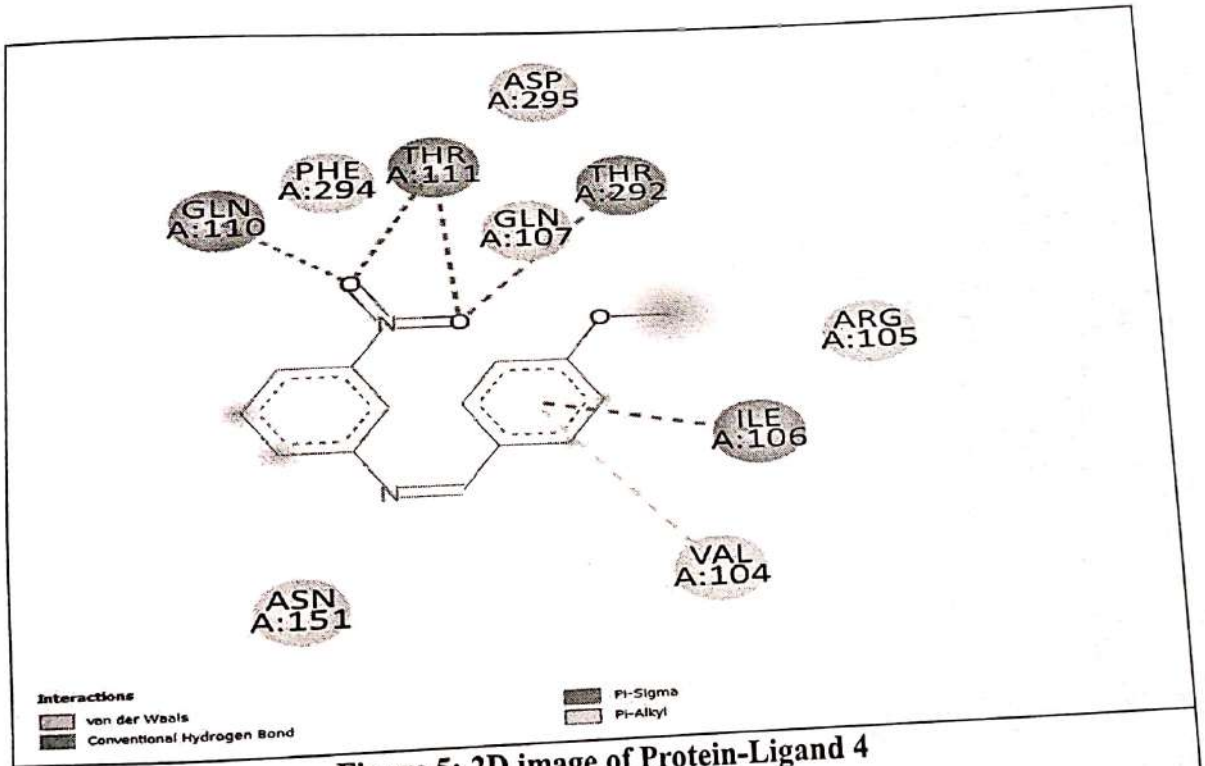


**Figure 5: 2D image of Protein-Ligand 4 interaction**

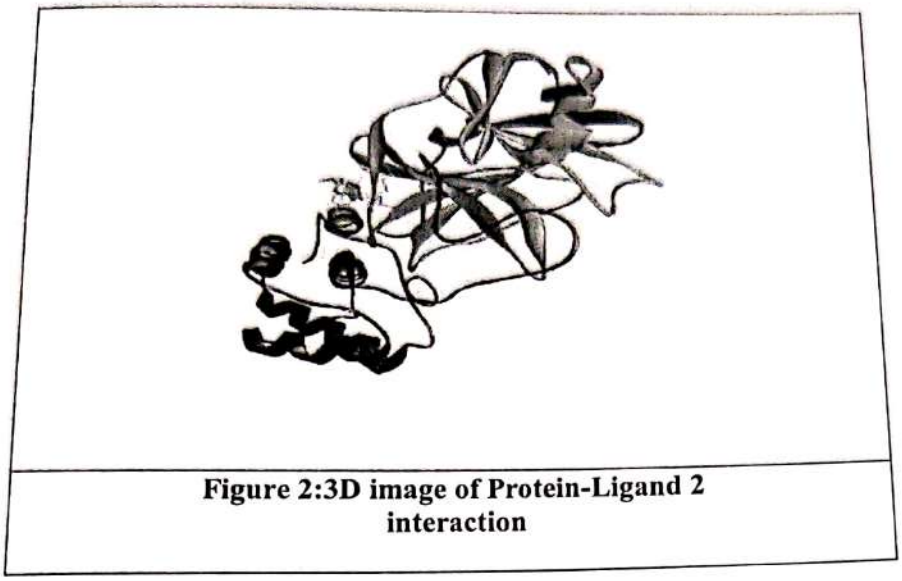

**Figure 2:3D image of Protein-Ligand 2 interaction**

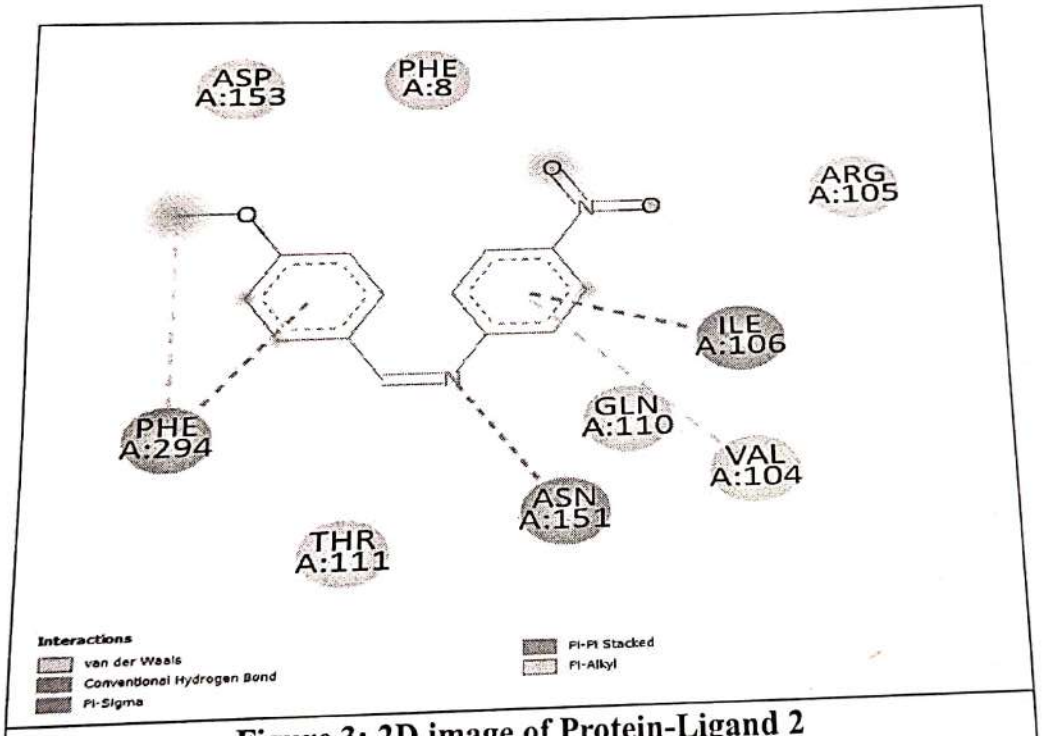


**Figure 3: 2D image of Protein-Ligand 2 interaction**

# *In-silico* Antidiabetic Activity of Bioactive Compounds In Pterocarpus Marsupium

**Mini Project**

Submitted in partial fulfillment of the

Requirement for the degree of

Bachelor of Pharmacy

**In**

The Faculty of Science & Technology,

Rashtrasant Tukadoji Maharaj Nagpur University, Nagpur.

**By**

**Miss. Shruti M. Kale**
B.Pharm.

**Guide**

**Mr. Kishor Danao**
M.Pharm., DDP.

Ambe Durga Education Society's

Dadasaheb Balpande College of Pharmacy, Besa,

Nagpur – 440037

2020-2021

**Research methodology –**

### 1. Selection of protein and preparation of its structure

Three dimensional crystal structure of Alpha amylase (PDB ID: 1UD6) involve in type II diabetes were downloaded in pdb format from the RCSB protein data bank (www.rcsb.org) with R value 2.50 Å, R-value free 0.250, R-value work 0.212 was selected for present study. Structure of the protein target were prepared and refined using digital studio visualizer 2021. The necessary hydrogen atoms were added. All solvent molecules and co-crystalized ligands were removed from structure in order to use as a receptor for docking by removing the water not involved in ligand binding and ligand molecules, inserting missing atoms, and correcting the valancies.

### 2. Selection of ligands and preparation of its structure

A total of 5 ligands of pterocarpus mauritiana were selected by literature survey and used for present study. They include epicatechin, pterostilbene, marsupin, liquirtigenin, pterosupin respectively. The 2D sdf format were downloaded from pubchem database (pubchem.ncbi.nlm.nih.gov). Energy minimization, geometrical confirmation and ydrogen bond is supplemented by pyrx-virtual screening tool.

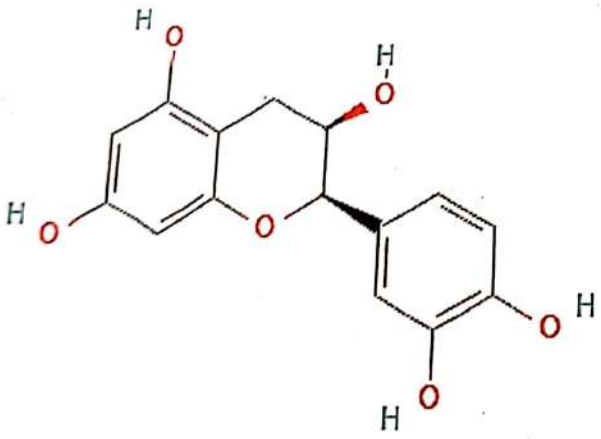

Fig A: (-)-Epicatechin

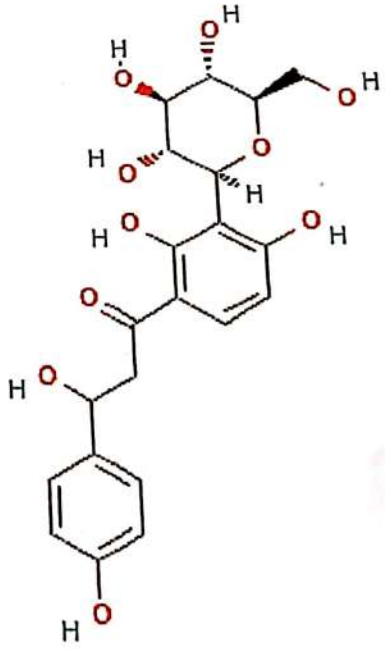

Fig B: pterosupin

### 3. Molecular properties and ligand based ADME/T analysis

The molecular properties of compounds play crucial role on the selection of these agents as potential drug candidates. SwissADME and protox-II is useful parameter to evaluate molecular properties of drug compounds for estimation of important pharmacokinetic parameters for drug design and development. SwissADME was used to screen the ligands as drug candidates, which states that the compound has more permeability and passive absorption if it does not violate more than one of the following conditions:(i) molecular weight (acceptable range: <500); (ii) hydrogen bond donor (acceptable range: ≤5); (iii) hydrogen bond acceptor (acceptable range: ≤10); (iv) high lipophilicity (expressed as log Po/w, acceptable range: <5); (v) molar refractivity should be between 40 and 130. The canonical SMILES for each compound is retrieved from PubChem and analysis was done through swissADME online database.

### 4. Receptor grid preparation

Receptor matrices were computed for arranged protein to such an extent that different ligand presents tie inside the anticipated active site during docking. Grids were created keeping the default parameters. A cubic box of particular measurements revolved around the centroid of active site buildups (reference ligand active site) was created for receptor for docking tests, the bouncing box was set to centre: X=9.4499, Y=84.1866, Z=100.1695

Dimension: X=50.9778, Y=78.7997, Z=66.7261

## Result & Discussion -

In order to study interaction of the compounds (-) epicatechin (CID 72276), pterostilbene (CID 5281727), marsupsin (CID 134369), liquirtigenin (CID 114829), pterosupin (CID 133775) with α-amylase, we performed docking analysis by pyrx-virtual screening tool, where among these compounds pterosupin shows highest docking score in table 1. The negative and low value of free energy of binding demonstrate a strongly favorable bond between α-amylase and pterosupin, due to the acceptable limits of hydrogen bond donor and hydrogen bond acceptor (-)epicatechin is most favorable conformation.

The aim of molecular docking is the accurate prediction of the structure of ligand within the constraints of receptor binding site and correctly estimate the strength of binding. The binding mode of pancreatic Alpha-Amylase with carbohydrate inhibitor (PDB 1UD6) was investigated by doing by doing computational analysis, docking. The result of docking analysis were describe in table 1 and the docking figure were shown. Among all the compounds (-)epicatechin showed the well docking score. Because the negative and low value of free energy of binding demonstrate a strongly favorable bond is preferable for best docking study. So the docking score between α-amylase in most favorable conformations.

Table 2 – ADME study of phytoconstituents of Pterocarpus marsupium

| Sr. No. | Molecule | Pubchem CID | Molecular Weight | HBA | HBD |
|---|---|---|---|---|---|
| 1 | Pterosupin | 133775 | 436.41 g/mol | 10 | 8 |
| 2 | (-)-Epicatechin | 72276 | 290.27 g/mol | 6 | 5 |
| 3 | Liquirtigenin | 114829 | 256.25 g/mol | 4 | 2 |
| 4 | Marsupsin | 134369 | 302.28 g/mol | 6 | 3 |
| 5 | Pterostilbene | 5281727 | 256.30 g/mol | 3 | 1 |

| Sr. No. | Molecule | Molar refractivity | ilogP | Total polar surface area |
|---|---|---|---|---|
| 1 | Pterosupin | 105.78 | 2.35 | 188.14 Å. |
| 2 | (-)-Epicatechin | 74.33 | 1.47 | 110.38 Å. |
| 3 | Liquitigenin | 69.55 | 1.73 | 66.76 Å. |
| 4 | Marsupsin | 77.24 | 1.20 | 96.22 Å. |
| 5 | Pterostilbene | 76.82 | 3.02 | 38.69 Å. |

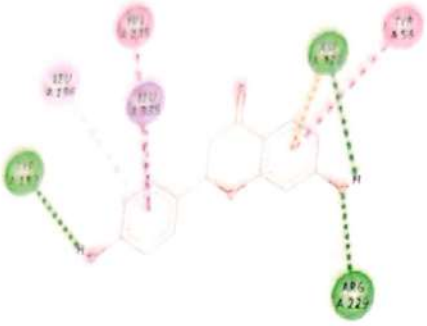

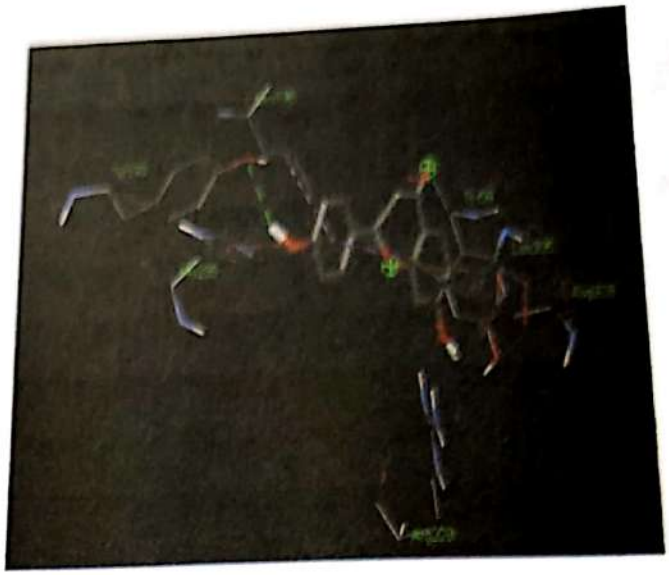

**Liquitigenin**

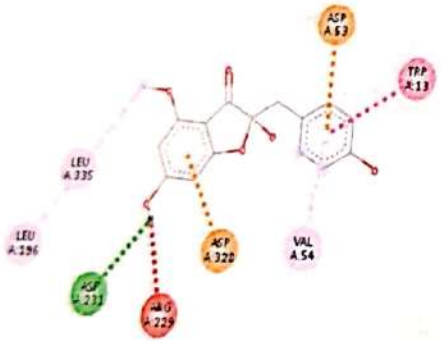


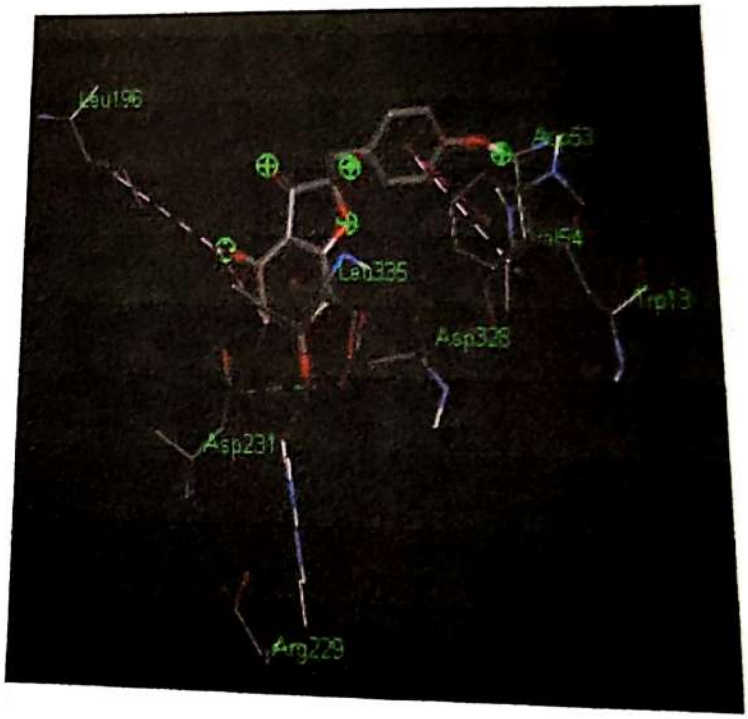


**Marsupsin**

**Ramachandran plot-**

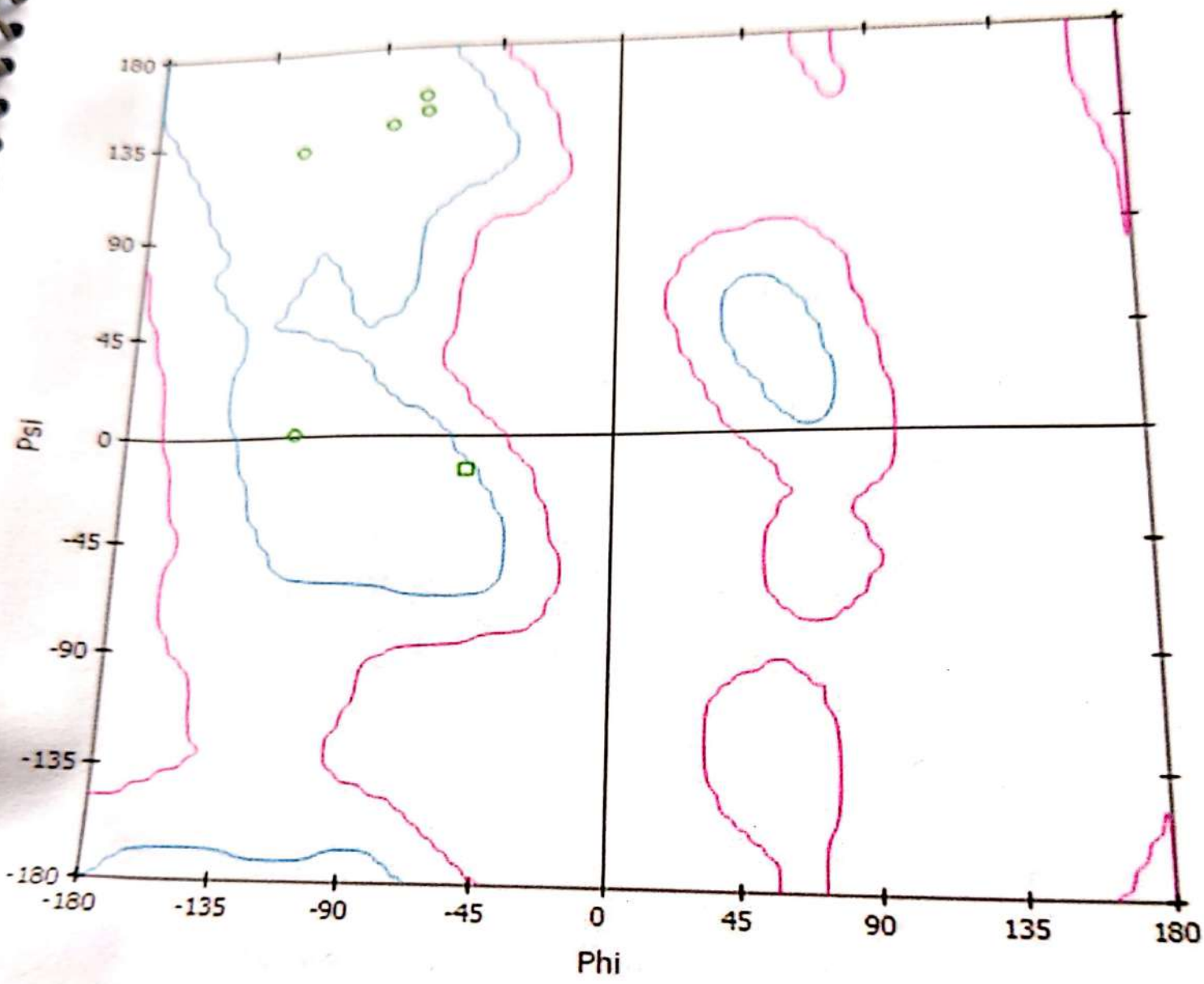


*Fig 3. Ramachandran plot showing allowed region in protein α-Amylase*

(354)

# Computational guided identification of potential phytoconstituent of plant *Withania Coagulans*

Submitted in partial fulfilment of the

Requirement for the degree of

**Bachelor of Pharmacy**

In the faculty of Science and Technology,

RashtrasantTukadojiMaharaj Nagpur University, Nagpur.

**By**

**Ms. Shruti V. Tejekar**

**Guide**

**Mr. Kishor R.Danao**

(M Pharm, DDP)



**AmbeDurga Education Society's**

**DadasahebBalpande College of Pharmacy, Besa,**

**Nagpur-440037 2021-**

**2022**

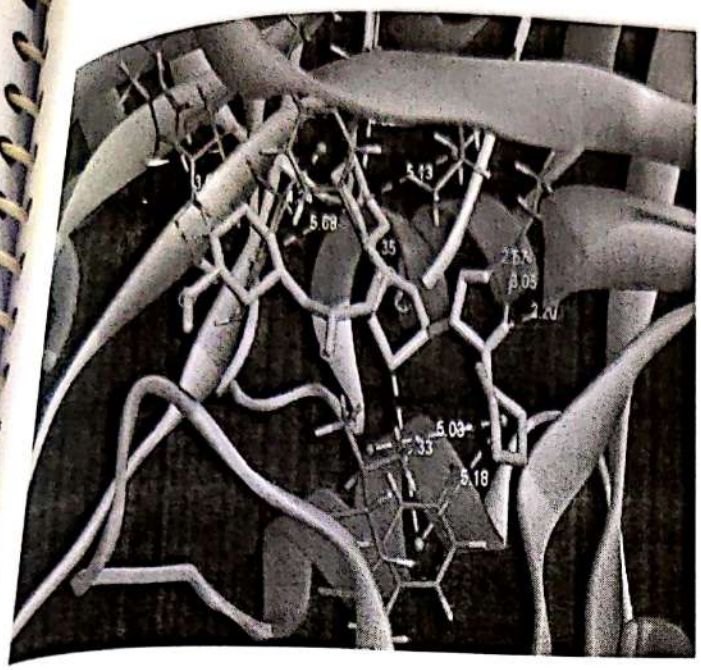


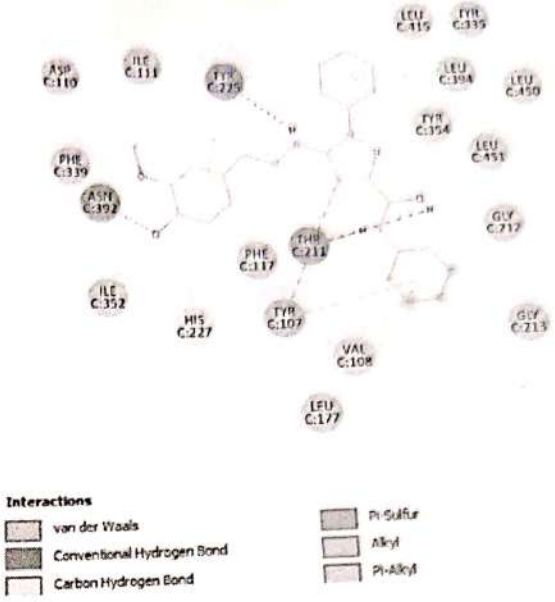


Figure no. (4) 2D & 3D Structure of 7KPB

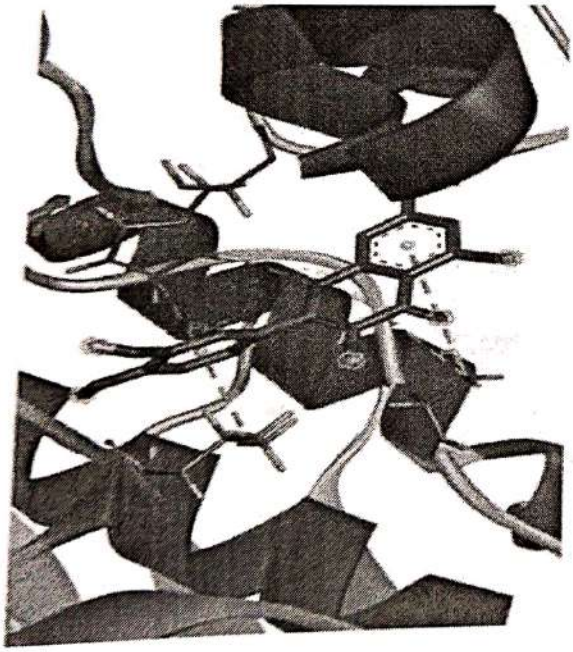

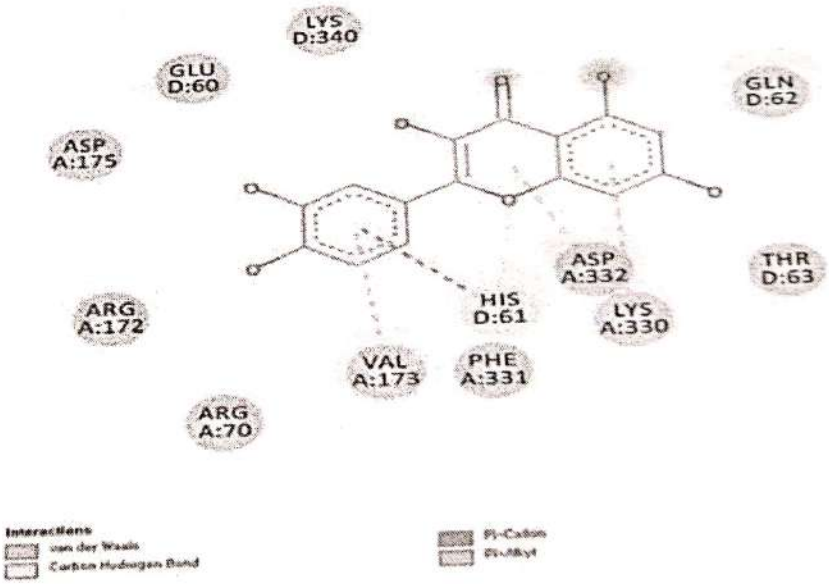


Figure no . (5) 2D & 3D Structure of 3WD5

# Development and Characterization of Gel Formulation for Topical Application

A THESIS

*Submitted to*

*Rashtrasant Tukadoji Maharaj Nagpur University, Nagpur*

*In partial fulfillment of the requirement for the award of the degree of*

**MASTER OF PHARMACY IN PHARMACEUTICS**

**In**

**FACULTY OF SCIENCE AND TECHNOLOGY**


**Submitted By**

**Mr. Kapil R. Pawar**

**Under the Guidance of**

**Dr. Purushottam S. Gangane**

M. Pharm, Ph.D.




**Dadasaheb Balpande College of Pharmacy,**

**Besa, Nagpur-440037**


**2021-2022**

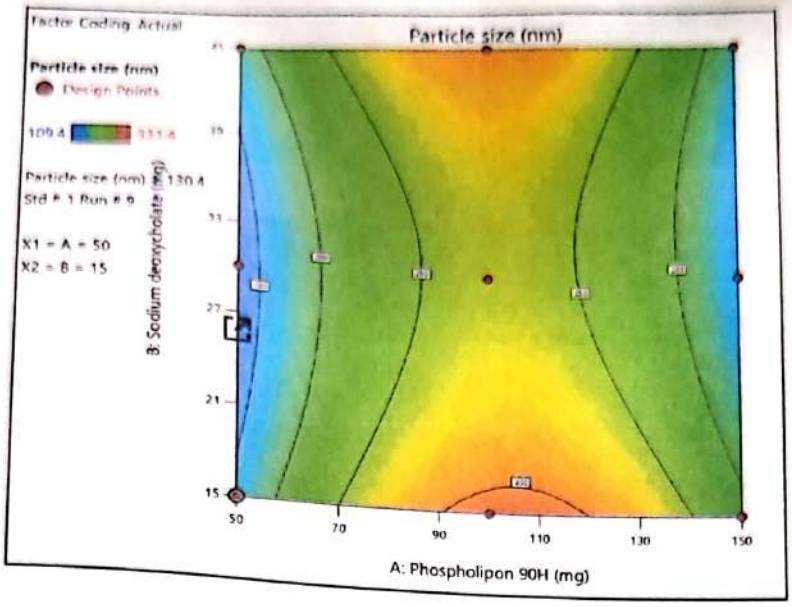


**Fig.20: Contour plot showing the effect of phospholipon®90H conc. with respect to Sodium deoxycholate conc. over the particle size.**

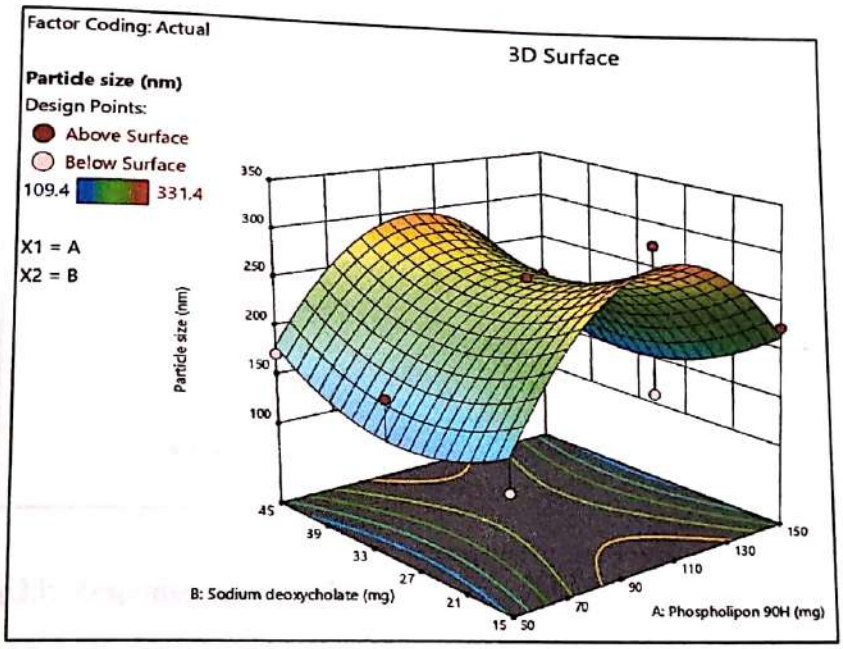


**Fig.21: Response surface plot showing the effect of Phospholipon®90H conc. with respect to Sodium deoxycholate conc. over the particle size.**

The contour plot shows predicted PDI values at different levels of Phospholipon®90H onc. and Sodium deoxycholate Conc. (Fig 22-23).

# FORMULATION DEVELOPMENT AND EVALUATION OF GASTRORETENTIVE FLOATING PELLETS FOR THE IMPROVEMENT OF BIOAVAILABILITY

**A THESIS**

*Submitted to*

*Rashtrasant Tukadoji Maharaj Nagpur University, Nagpur*

*In partial fulfillment of the requirement for the award of the degreeof*

**MASTER OF PHARMACY IN PHARMACEUTICS**

**in**

**FACULTY OF SCIENCE AND TECHNOLOGY**


**Submitted By**

**MR. RUSHIKESH A. HARDE**

**Guide**

**DR. NILESH M. MAHAJAN**

M. Pharm, Ph.D.




**Dadasaheb Balpande College of Pharmacy,**

**Besa, Nagpur-440037**


**2021-2022**

## 6.4 SOLUBILITY STUDY

Saturated solubility studies were carried out using 2 different solvents, i.e., distilled water and 0.1N HCl. The primary objective of using various mentioned solvents was to determine which solvents were the most suitable for enhanced released LSH loaded floating pellets. Saturated solutions were prepared by adding excess pure lurasidone hydrochloride in to a small vial containing 10 ml of 0.1N HCl. The sample was then left in a bath shaker for 48 h under a constant room temperature and shaking speed of 40 rpm. The supernatant was then filtered and diluted with 0.1N HCL solution. This was then analyzed via a UV spectrophotometer at a wavelength 227 nm to determine the concentration of lurasidone hydrochloride in each sample.[4]

## 6.5 PREPARATION AND OPTIMIZATION OF LURASIDONE HYDROCHLORIDE GASTRORETENTIVE FLOATING PELLETS

Gastroretentive floating pellets of lurasidone hydrochloride were prepared by using extrusion spheronization technique followed by fluidized bed dryer. Drug, HPMC K100M, EC, sodium bicarbonate, microcrystalline cellulose, PVP K-30, talc, and magnesium stearate were sifted through sieve no. 40 and accurately weighed. The excipients were blended in geometric fashion, using cone blender for 10 min. Water was gradually added to the powder blend. The dough mass was extruded through mini screw extruder (1 mm pore size) at speed of 20 to 40 rpm. The extrudates were collected. Extrudates were spheronized at variable speed which is 750, 800, 850 rpm for 15 min. The obtained pellets were dried at 70°C for 10 min in a Fluidized bed dryer.

### 6.5.1 EXPERIMENTAL DESIGN

A 3-level. 3-factor, 13-run experimental Box-Behnken design was adopted to optimize levels of variables in the pellet formulations. The selected independent variables were concentration of HPMC K100, i.e., Hydroxypropyl Methylcellulose (X1), concentration of EC, i.e. Ethyl Cellulose (X2), and spheronizing speed (X3) as shown in Table 1. The dependent variables were % drug release (Y1), aspect ratio (Y2) friability (Y3). The generation of experimental runs, ANOVA study and optimization were carried out by Design-expert software 13. The formulation batches prepared are indicated in (Table 6.4).

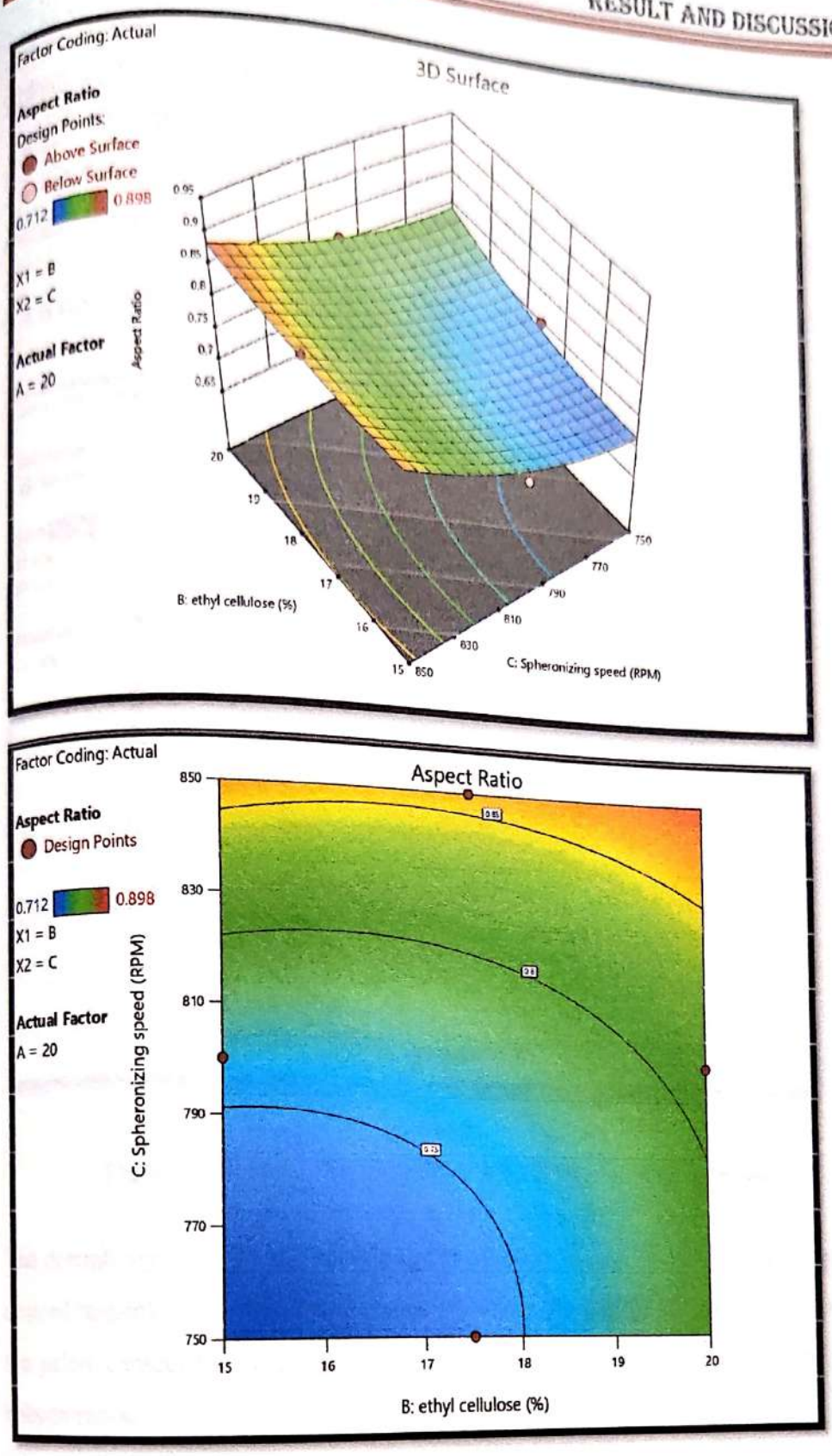


**Fig no. 29 Contour plot and 3D surface response plot showing effect of ethyl cellulose vs spheronizing speed on aspect ratio**

# FORMULATION OF POLYHERBAL EMULGEL BY QUALITY BY DESIGN (QbD) APPROACH FOR ALOPECIA

Thesis

Submitted in partial fulfilment of the

Requirements for the degree of

**Masters of Pharmacy**

**In**

**Pharmaceutical Quality Assurance**

In the Faculty of Science and Technology,

Rashtrasant Tukdoji Maharaj Nagpur University, Nagpur

Submitted by

**Mr. Tirupati G. Kedar**

Under the Guidance of

**Dr. (Mrs). Ujwala N. Mahajan**

Ambe Durga Education Society's

Dadasaheb Balpande College of Pharmacy, Besa, Nagpur-440037

2021-2022

| | | |
|---|---|---|
| Preservative (Methylparaben:propylparaben: Carbopol 934 | 2:1 (0.3:0.2) | 4:2 (0.6:0.2) |
| Permeation Enhancer Oleic acid | 0.5 gm | 1gm |
| Triethanolamine | 0.5gm | 1gm |
| Water | q.s | q.s |
| | 50 ml | 100 |

## 6.11 SYSTEMATIC OPTIMIZATION OF POLYHERBAL EMULGEL:

The systematic optimization of polyherbal emulgel was carried out using Box-Behnken design (BBD) with the help of Design Expert® ver. 13.0 software (Stat-Ease Inc., Minneapolis, USA).Three most influential factors including concentration of Carbopol 934, concentration Cremophore A25, and concentration, Oleic Acid were selected as independent variables (factors) for optimization at three different levels, viz., low (-1), medium (0) and high (+1). Atotal of 14 experimental trials were suggested by the selected design as shown in Table 6.6. Surface Plasmon Resonance and percentage Entrapment efficiency formulation of polyherbal emulgel were analyzed as responses. After putting the data in BBD, mathematical modelling was performed to analyze the results. Quadratic second-order model was selected and the data-fitting with the model was analyzed by ANOVA along with other parameters like coefficient of correlation ($r^2$), adjusted $r^2$, predicted $r^2$ and predicted residual sum of squares. *Phyllanthus embilica,( fruit) Hibiscus rosa sinensis,(flower) and Nigella sativa (seeds)* extract Optimized conditions required for polyherbal emulgel formulation were identified by the numerical desirability function and graphical optimization techniques.[135]

**Table No. -6.4 Experimental Factors for Polyherbal Emulgel and Corresponding Levels** [84]

| Independent Variables | Variable Levels | | |
|---|---|---|---|
| | Low (-1) | Medium (0) | High (+1) |
| Concentration of Carbopol 934 | 0.5 | 0.75 | 1 |
| Concentration of Cremophore A25 | 2.5 | 3.5 | 2.5 |
| Concentration of Oleic Acid | 0.1 | 1.75 | 2.5 |

**Table No. 6.5: Details of design runs for synthesis of polyherbal emulgel with the corresponding responses.**

| Runs | Concentration of Carbopol 934 | Concentration of Cremophore A25 | Concentration of Oleic Acid |
|---|---|---|---|
| 1 | 0.5 | 2.5 | 1.3 |
| 2 | 1 | 2.5 | 1.3 |
| **3** | **0.5** | **5** | **1.3** |
| 4 | 1 | 5 | 1.3 |
| 5 | 0.5 | 3.75 | 0.1 |
| 6 | 1 | 3.75 | 0.1 |
| 7 | 0.5 | 3.75 | 2.5 |
| 8 | 1 | 3.75 | 2.5 |
| 9 | 0.75 | 2.5 | 0.1 |
| 10 | 0.75 | 5 | 0.1 |
| 11 | 0.75 | 2.5 | 2.5 |
| 12 | 0.75 | 5 | 2.5 |
| 13 | 0.75 | 3.75 | 1.3 |
| 14 | 0.75 | 3.75 | 3.75 |
| 15 | 0.75 | 3.75 | 3.75 |

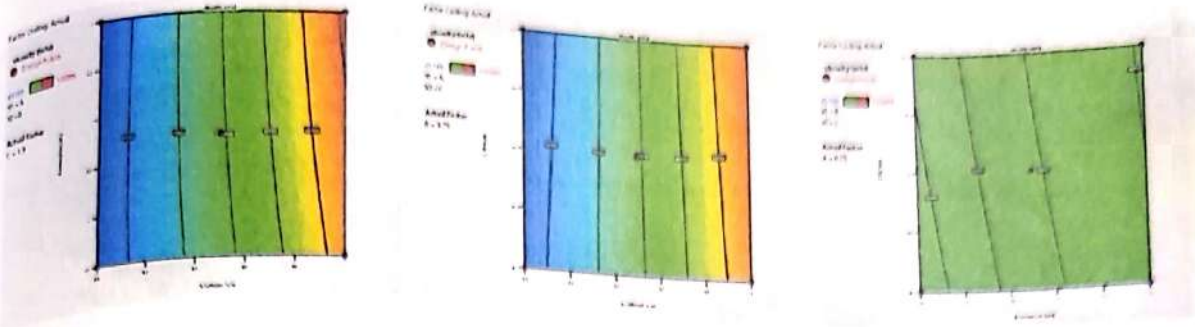

**Fig no. 7.15: Contour plot showing effect of independent variables on viscosity of emulgel formulation**

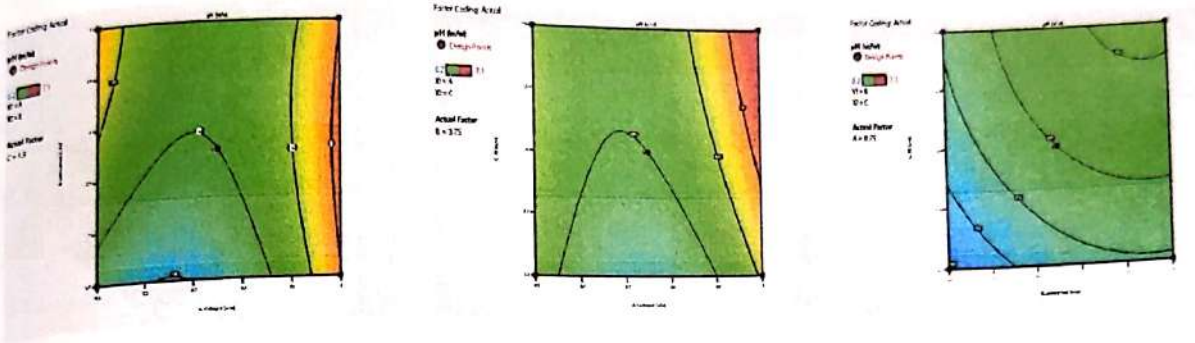

**Fig no. 7.16: Contour plot showing effect of independent variables on pH of emulgel formulation**

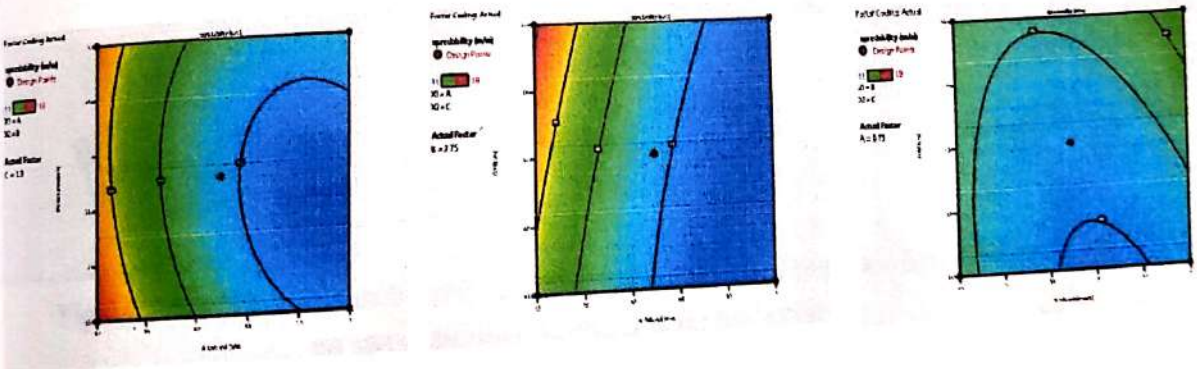

**Fig no. 7.17: Contour plot showing effect of independent variables on spreadability of emulgel formulation.**

# A PANCHAGAVYA-BASED HERBAL NANOGEL WITH POTENTIAL FOR PSORIASIS

**A THESIS**

Submitted to

*Rashtrasant Tukadoji Maharaj Nagpur University, Nagpur*

*In partial fulfillment of the requirements for the degree of*

**MASTER OF PHARMACY IN PHARMACEUTICS**

in

**FACULTY OF SCIENCE & TECHNOLOGY**


Submitted by,

**Mr. Tushar R. Mandale**

B.Pharm.

Guided by,

**Dr. Nilesh M. Mahajan**

M.Pharm., Ph.D.




**DADASAHEB BALPANDE COLLEGE OF PHARMACY,**

**BESA, NAGPUR-440037 (MS)**


**2021-2022**

## 6.9 SYNTHESIS OF SILVER NANOPARTICLES:

1 gm of seeds extract was dissolved in 10 ml of ethyl acetate and the pH (9-11) was adjusted. The solution was heated at a temperature range of 60–80 °C and followed by addition of $AgNO_3$ solution with the help of burette at varying concentrations (0.01–0.10 M) with continuous stirring with the help of a magnetic stirrer. Formation of nanoparticles was identified by the colour change of solutions from yellow to brownish-yellow or deep brown. UV spectroscopy was used to examine the reaction mixture for the formation of silver nanoparticles (400-800 nm) [20].

### 6.9.1: PREPARATION OF SILVER NITRATE SOLUTION:

- **For 0.01 M:** 0.17 gm of silver nitrate dissolved in 100 ml of double distilled water.
- **For 0.05 M:** 0.85 gm of silver nitrate dissolved in 100 ml of double distilled water.
- **For 0.1 M:** 1.7 gm of silver nitrate dissolved in 100 ml of double distilled water.

### 6.9.2: PREPARATION OF 0.1 M NAOH AND HCL:

- **For 0.1 M NaOH:** 4.25 gm of NaOH dissolved in 100 ml of double distilled water.
- **For 0.1 M HCl:** 8.5 ml of HCl in 100 ml of double distilled water.

## 6.10: SYSTEMATIC OPTIMIZATION OF SILVER NANOPARTICLES:

The systematic optimization of silver nanoparticles was carried out using Box-Behnken design (BBD) with the help of Design Expert® ver. 13.0 software (Stat-Ease Inc., Minneapolis, USA). Three most influential factors including concentration of silver nitrate, temperature and pH were selected as independent variables (factors) for optimization at three different levels, viz., low (-1), medium (0) and high (+1). A total of 14 experimental trials were suggested by the selected design as shown in Table 6.4. Surface Plasmon Resonance and percentage entrapment efficiency of synthesized silver nanoparticles were analyzed as responses. After putting the data in BBD, mathematical modelling was

performed to analyze the results. Quadratic second-order model was selected and the data-fitting with the model was analyzed by ANOVA along with other parameters like coefficient of correlation $r^2$, adjusted $r^2$, predicted $r^2$ and predicted residual sum of squares. Optimized conditions required for silver nanoparticle synthesis were identified by the numerical desirability function and graphical optimization techniques [24].

**Table No. 6.3: Experimental factors for biosynthesis of AgNPs and corresponding levels**

| Independent Variables | Variable Levels | | |
|---|---|---|---|
| | Low (-1) | Medium (0) | High (+1) |
| Concentraion of silver nitrate (M) | 0.01 | 0.05 | 0.1 |
| Temperature (°C) | 60 | 70 | 80 |
| pH | 9 | 10 | 11 |

**Table No. 6.4: Details of design runs for synthesis of AgNPs with the corresponding responses**

| Runs | Concentration of silver nitrate (M) | Temperature (°C) | pH |
|---|---|---|---|
| 1 | 0.05 | 80 | 9 |
| 2 | 0.01 | 80 | 10 |
| 3 | 0.05 | 60 | 9 |
| 4 | 0.1 | 80 | 10 |
| 5 | 0.05 | 80 | 11 |
| 6 | 0.05 | 70 | 10 |
| 7 | 0.1 | 70 | 11 |
| 8 | 0.01 | 70 | 9 |
| 9 | 0.1 | 60 | 10 |
| 10 | 0.01 | 60 | 10 |

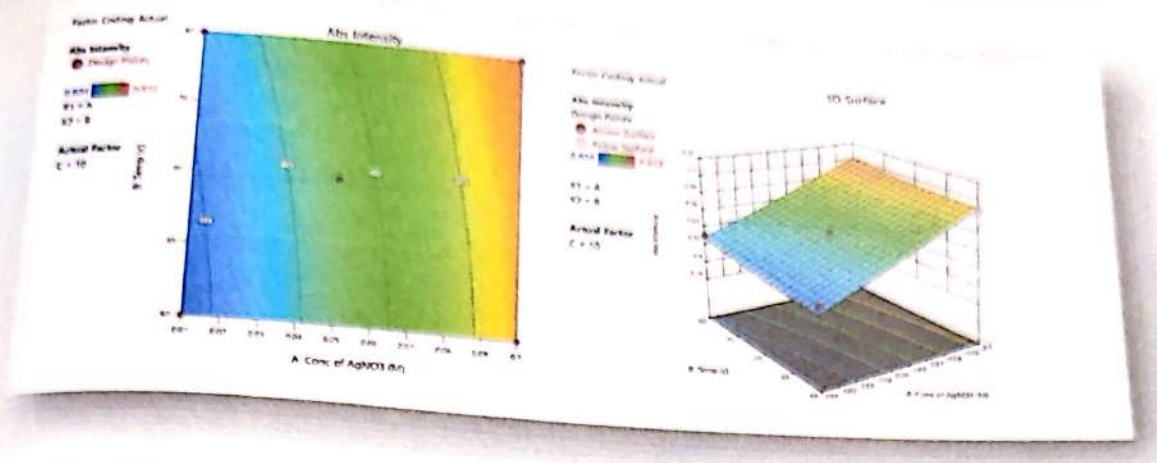


**Fig No. 7.9: Contour plot and 3D-Response surface plot showing effect of concentration of silver nitrate and temperature on absorbance intensity**

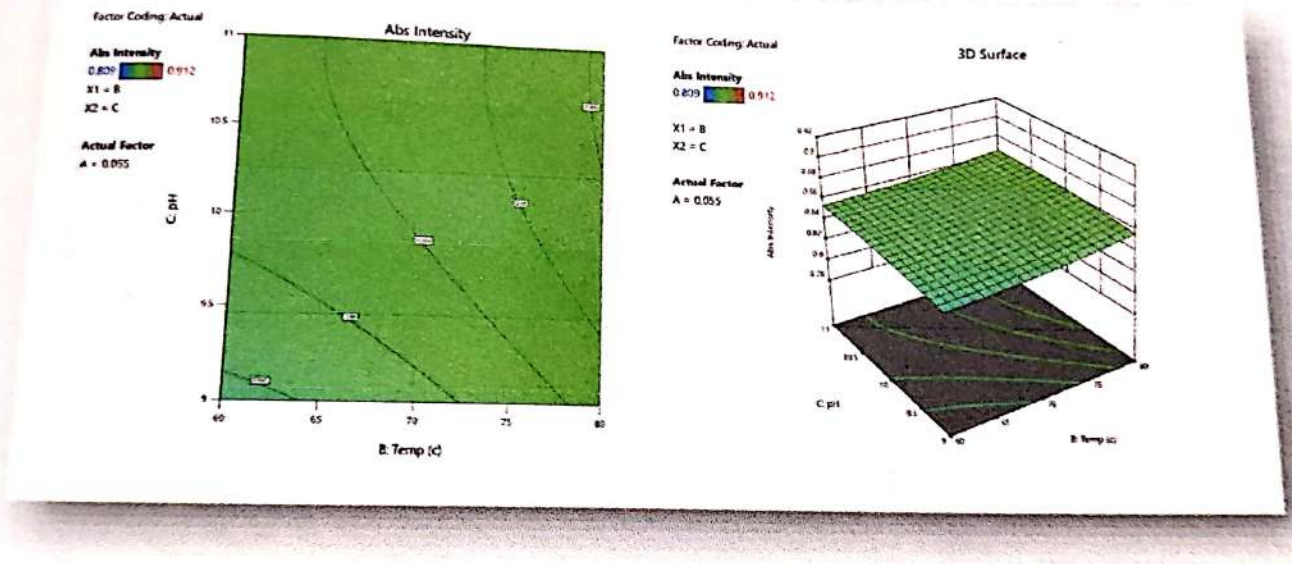


**Fig No. 7.10: Contour plot and 3D-Response surface plot showing effect of pH and temperature on absorbance intensity**

AAPS PharmSciTech (2022) 23:177
https://doi.org/10.1208/s12249-022-02315-8

RESEARCH ARTICLE

Theme: Recent Advances on Drug Delivery Systems for Viral Infections

# Improvement in Bioavailability and Pharmacokinetic Characteristics of Efavirenz with Booster Dose of Ritonavir in PEGylated PAMAM G4 Dendrimers

Rohini Kharwade[1] · Sachin More[1] · Elizabeth Suresh[1] · Amol Warokar[1] · Nilesh Mahajan[1] · Ujwala Mahajan[1]

Received: 11 March 2022 / Accepted: 25 May 2022


## Abstract

Efavirenz (EFV) with a booster dose of ritonavir (RTV) (EFV-RTV) inhibits the metabolism of EFV and improves its bioavailability. However, inadequate organ perfusion with surface permeability glycoprotein (P-gp) efflux sustains the viable HIV. Hence, the present investigations were aimed to evaluate the pharmacokinetics and tissue distribution efficiency of EFV by encapsulating it into PEGyalated PAMAM (polyamidoamine) G4 dendrimers with a booster dose of RTV (PPG4ER). The entrapment efficiency of PEGylated PAMAM G4 dendrimers was found to be 94% and 92.12% for EFV and RTV respectively with a zeta potential of 0.277 mV. The pharmacokinetics and tissue distribution behavior of EFV within PPG4ER was determined by developing and validating a simple, sensitive, and reliable bioanalytical method of RP-HPLC. The developed bioanalytical method was very sensitive with a quantification limit of 18.5 ng/ml and 139.2 ng/ml for EFV and RTV, respectively. The comparative noncompartmental pharmacokinetic parameters of EFV were determined by administrating a single intraperitoneal dose of EFV, EFV-RTV, and PPG4ER to Wistar rats. The PPG4ER produced prolonged release of EFV with a mean residential time (MRT) of 24 h with $C_{max}$ 7.68 µg/ml in plasma against EFV-RTV with MRT 11 h and $C_{max}$ 3.633 µg/ml. The PPG4ER was also detected in viral reservoir tissues (lymph node and spleen) for 3–4 days, whereas free EFV and EFV-RTV were cleared within 72 h. The pharmacokinetic data including $C_{max}$, $t_{1/2}$, $AUC_{tot}$, and MRT were significantly improved in PPG4ER as compared with single EFV and EFV-RTV. This reveals that the PPG4ER has great potential to target the virus harbors tissues and improve bioavailability.

**KEY WORDS** efavirenz · ritonavir · bioanalytical method · pharmacokinetic · bioavailability

## INTRODUCTION

Due to the emergence of resistant strains of the human immune virus (HIV) and the presence of viral reservoirs, antiretroviral therapy (ART) with any single class of drug has proven ineffective in controlling the infection and disease progression (1). Disease management is also challenging due to less bioavailability, and side effects of ART drugs (2, 3). The approaches to target the viral reservoir, and resolve the complications of current ART include the invention of novel drug molecules, chemical modifications of ART, altered drug regimens, activation of the immune system, and development of targeted drug delivery systems (4). Out of these, PAMAM dendrimers revolutionized ART by improving the delivery and efficacy of ART drugs.

In consideration of the new drug regimen, EFV is a first-choice non-nucleoside reverse transcriptase inhibitor used in ART. Unfortunately, it induces P4502B6 enzymes,

Guest Editor: Claudio Salomon

✉ Rohini Kharwade
rohinismore1@gmail.com

[1] Dadasaheb Balpande College of Pharmacy, Besa, Nagpur, Rashtrasant Tukadoji Maharaj Nagpur University, Nagpur, (MS) 440037, India

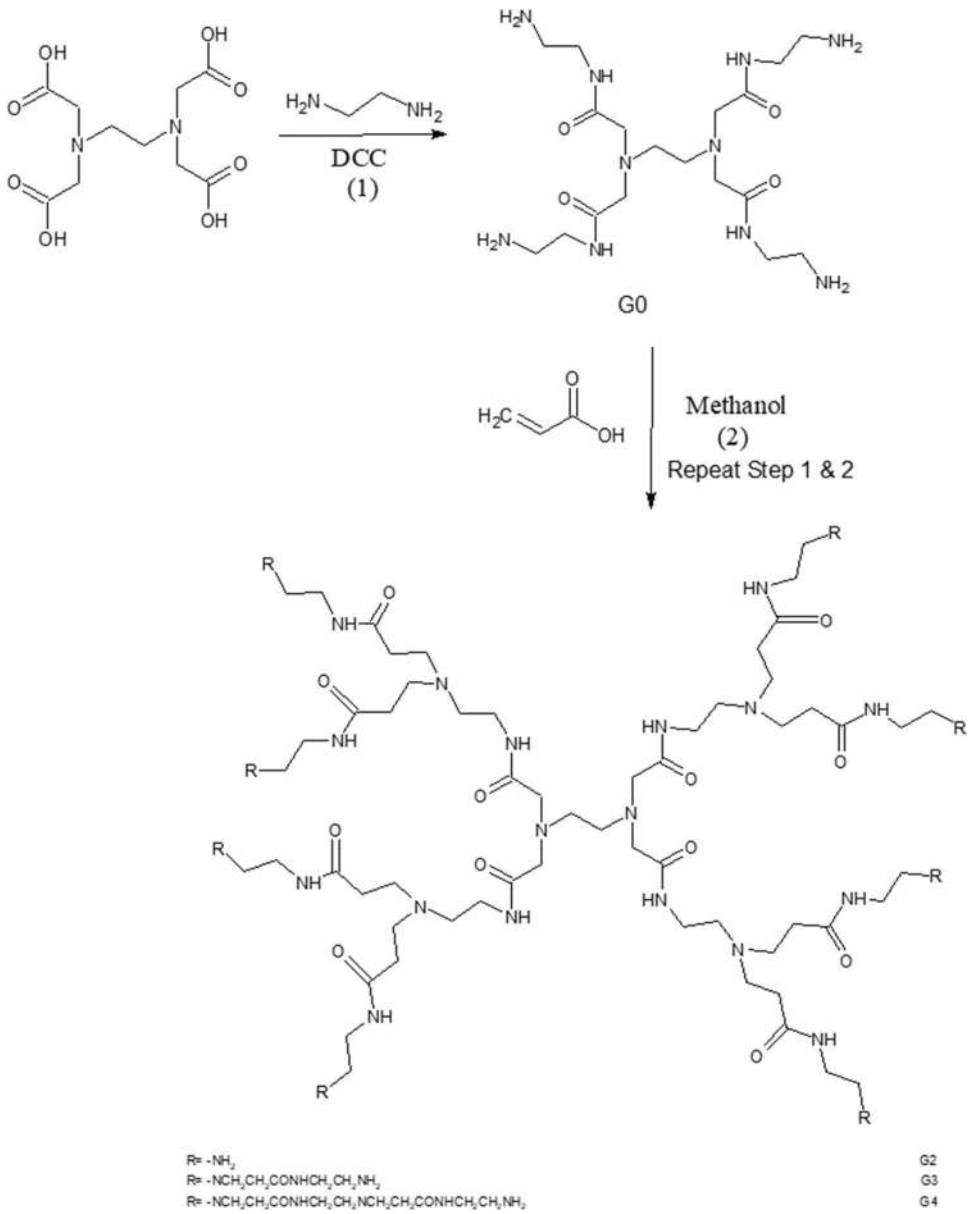


**Scheme 1** Divergent approach for synthesizing PAMAM G4 dendrimer by repetition of Michael addition and amidation with excess of reagent

(250 mm × 4.6 mm, 5 µm). Method development trials for HPLC analysis were carried out by isocratic mode using ammonium acetate buffer (25 mM) at various pH (pump A). Different percentage ratios of methanol: acetonitrile were used for pump B. Various chromatographic trials were conducted by altering the composition of the mobile phase, pH, and flow rate for the resolution of peaks (34, 35).

### Sample Extraction Procedure

Blood samples were withdrawn from the retro-orbital plexus of the rat and placed into anti-clot blood collection vials (Himedia Laboratories, Mumbai, India). Subsequently, the withdrawn blood samples were instantaneously centrifuged at 12,000 rpm for 10 min (4 °C) and the supernatant was decanted as a plasma (36, 37). The tissue distribution study was performed on various tissues like the heart, liver, kidney, spleen, brain, and cervical lymph node. These tissues were harvested and rinsed with ice-cold 0.9% NaCl to remove superficial blood and debris. Further, the tissues were dried by blotting with filter paper. Each tissue was accurately measured and homogenized with 3 times its volume with methanol. These plasma/tissue homogenates are stored in vials at − 20 °C until further investigation and proceed for single-step protein precipitation by liquid–liquid extraction (38).

### Liquid–Liquid Extraction

In an eppendorf tube, aliquots of 100 µL of rat plasma/tissue homogenates were treated with 1 mL of working solution for

as well as tissue compartments as compared to EFV-RTV. Therefore, it has been concluded that PPG4ER dendrimers could be a promising candidate to target the virus harbors tissues and improve bioavailability.

**Author Contribution** Rohini Kharwade and Elizabeth Suresh completed experimental works and drafted the manuscript. Dr. Amol Warokar and Sachin More gave supporting investigation and discussion in a pharmacokinetic study. Dr. Nilesh Mahajan gave productive suggestions and experimental instruction and Dr. Ujwala Mahajan supervised.

## Declarations

**Conflict of Interest** The authors declare no competing interests.

## References


1. Shuh M, Beilke M. The human T-cell leukemia virus type 1 (HTLV-1): new insights into the clinical aspects and molecular pathogenesis of adult T-Cell leukemia / lymphoma (ATLL) and tropical spastic paraparesis/HTLV- associated myelopathy (TSP/HAM). Macro Res Tech. 2005;196(March):176–96.
2. Desai M, Iyer G, Dikshit RK. Antiretroviral drugs : critical issues and recent advances. Ind J Pharmacol. 2012;44(3):288–96.
3. Piketty C, Race E, Castiel P, Belec L, Peytavin G, Si-mohamed A, *et al*. Efficacy of a five-drug combination including ritonavir, saquinavir and efavirenz in patients who failed on a conventional triple-drug regimen : phenotypic resistance to protease inhibitors predicts outcome of therapy. AIDS. 1999;13(11):71–7.
4. Lembo D, Donalisio M, Civra A, Argenziano M, Lembo D, Donalisio M, *et al*. Expert opinion on drug delivery nanomedicine formulations for the delivery of antiviral drugs : a promising solution for the treatment of viral infections. Expert Opin Drug Deliv [Internet]. 2018;15(1):93–114. Available from: https://doi.org/10.1080/17425247.2017.1360863
5. Barry M, Mulcahy F, Merry C, Gibbons S, Back D. Pharmacokinetics and potential interactions amongst antiretroviral agents used to treat patients with HIV infection. Clin Pharmacokinet. 1999;36(4):289–304.
6. Kappelhoff BS, Crommentuyn KML, De Maat MMR, Mulder JW, Huitema ADR, Beijnen JH. Practical guidelines to interpret plasma concentrations of antiretroviral drugs. Clin Pharmacokinet. 2004;43(13):845–53.
7. Adkins JC, Noble S. Efavirenz Drugs. 1998;56(6):1055–64.
8. Parienti JJ, Ragland K, Lucht F, De La Arnaud B, Dargàre S, Yazdanpanah Y, *et al*. Average adherence to boosted protease inhibitor therapy, rather than the pattern of missed doses, as a predictor of HIV RNA replication. Clin Infect Dis. 2010;50(8):1192–7.
9. Margolis L, Shattock R. Selective transmission of CCR5-utilizing HIV-1: the 'gatekeeper' problem resolved? Nat Rev. 2006;4(April):312–7.
10. John Gill, Charlotte Lewden, Mike Saag PR. Causes of death in HIV-1 – infected patients treated with antiretroviral therapy , 1996 – 2006 : collaborative analysis of 13 HIV cohort studies. Clin Inf Dis. 2010;50(10):1387–96.
11. Kharwade R, More S, Mahajan N, Agrawal P. Functionalised dendrimers: potential tool for antiretroviral therapy. Curr Nanosci. 2020;16(5):708–22.
12. Gupta S, Kesarla R, Chotai N, Omri A. Development and validation of reversed- phase HPLC gradient method for the estimation of efavirenz in plasma. Plos One. 2017;1–12.
13. Kraft JC, Mcconnachie LA, Koehn J, Sun J, Collier AC, Collins C, *et al*. Mechanism-based pharmacokinetic (MBPK) models describe the complex plasma kinetics of three antiretrovirals delivered by a long-acting anti-HIV drug combination nanoparticle formulation John. J Cont Rel. [Internet]. 2018; Available from: https://doi.org/10.1016/j.jconrel.2018.02.003
14. Tomalia DA, Hall VB, Hall M, Hedstrand DM. Starburst dendrimers :covalently fixed unimolecular assemblages reiminiscent of spheroidal micelles. Macromolecules. 1987;20(5):1164–7.
15. Tomalia DA. Starburst™/cascade dendrimers: fundamental building blocks for a new nanoscopic chemistry set. Aldrichimica Acta. 1993;26(1):91–101.
16. Shadrack DM, Mubofu EB, Nyandoro SS. Synthesis of polyamidoamine dendrimer for encapsulating tetramethylscutellarein for potential bioactivity enhancement. Int J Mol Sci. 2015;26363–77.
17. Mario Ficker, Valentina Paolucci JBC. Improved large scale synthesis and characterization of small and medium generation PAMAM-dendrimers. Can J Chem. 2017;1–31.
18. Esfand R, Tomalia DA. Laboratory synthesis of poly(amidoamine) (PAMAM) dendrimers. Dendrimers Other Dendritic Polym. 2002;1:587–604.
19. Vögtle F, Gestermann S, Hesse R, Schwierz H, Windisch B. Functional dendrimers. Prog Polym Sci. 2000;25(7):987–1041.
20. Abbasi E, Aval SF, Akbarzadeh A, Milani M, Nasrabadi HT, Joo SW, *et al*. Dendrimers: synthesis, applications, and properties. Nanoscale Res Lett. 2014;9(1):1–10.
21. Kim Y, Klutz AM, Jacobson KA. Systematic investigation of polyamidoamine dendrimers surface-modified with poly(ethylene glycol) for drug delivery applications: synthesis, characterization, and evaluation of cytotoxicity. Bioconjugate Chem. 2008;19(ii):1660–72.
22. Anisha AD, Shegokar R. Expert opinion on drug delivery polyethylene glycol ( PEG ): a versatile polymer for pharmaceutical applications. Expert Opin Drug Deliv [Internet]. 2016;13(9):1257–75. Available from: https://doi.org/10.1080/17425247.2016.1182485
23. Qi R, Gao Y, Tang Y, He RR, Le LT, He Y, *et al*. PEG-conjugated PAMAM dendrimers mediate efficient intramuscular gene expression. AAPS J. 2009;11(3):395–405.
24. Pyreddy S, Kumar P, Kumar P. Polyethylene glycolated PAMAM dendrimers-efavirenz conjugates. Int J Pharm Investig. 2014;4(1):15.
25. Zhu S, Hong M, Zhang L, Tang G, Jiang Y, Pei Y. PEGylated PAMAM dendrimer-doxorubicin conjugates: in vitro evaluation and in vivo tumor accumulation. Pharm Res. 2010;27(1):161–74.
26. Khambete H, Jain NP, Jain CP. Effect of polyethylene glycol chain Length on PEGylation of dendrimers. Asian J Pharm. 2017;11(1):7–12.
27. Shadrack DM, Swai HS, Munissi JJE, Mubofu EB, Nyandoro SS. Polyamidoamine dendrimers for enhanced solubility of small molecules and other desirable properties for site specific delivery: Insights from experimental and computational studies. Molecules. 2018;23(6).
28. Zeng Y, Kurokawa Y, Hirano S. multiple generations on cytotoxicity and neuronal differentiation using Effects of PAMAM dendrimers with various surface functional groups and multiple generations on cytotoxicity and neuronal differentiation using human neural progenitor cells. J Toxic Sci. 2016;41(3):351–70.